Kingston University London

Submitted to the Division of Postgraduate Research

of Kingston University, London

The Role of ATM-INteracting protein (ATMIN) and Dishevelled associated activator of morphogenesis 2 (Daam2) proteins in kidney cell growth

This Thesis is submitted in Partial Fulfilment of the requirements of Kingston University for the Degree of:

Masters (MSc) by Research in Genetics

By: Shamaine Teandra KING (S.T.K)

March 2017

Supervisor:

Dr. Mark Carew

Associate Professor

Life Sciences, Pharmacy & Chemistry

Word Count: 10, 168

Abstract Word Count: 297

Total Word Count: 14859

Table of Contents **Page Number**

Abstract

Planar Cell Polarity (PCP) has emerged as an important pathway in organ development and tissue morphogenesis. PCP is responsible for the downstream cascades that cause cytoskeleton rearrangement changes because it directs the polarised alignment of cells perpendicular to the apical-basal axis. This causes asymmetric redistribution of core PCP proteins resulting in essential contributions in: ciliary positioning, cell shape regulation, branching morphogenesis and directional cell movement. PCP perturbation has resulted in serious morphological defects resulting in diseases such as Polycystic Kidney Disease (PKD).

Roles for multiple PCP genes have been discovered although the mechanisms by which the pathway operates are yet to be defined. ATM-INteracting protein (ATMIN) has proven to be important to the PCP pathway for its role in ciliogenesis, lung morphogenesis. This is due to the direct binding of ATMIN to DYNYLL1.DYNYLL 1 is an associated light chain of the dynein motor complex. It is required for

proper folding and dimerization of the cargo-binding dynein intermediate chain.

An additional role for ATMIN in kidney morphogenesis was found. A study by Goggolidou, et al., 2014 has shown that ATMIN Gasping6 embryonic mouse kidneys (resulting in ATMIN deficiency) show morphological abnormalities consistent with PCP pathway perturbation. Results also recorded changes in PCP proteins, most notably a two fold increase in Dishevelled associated activator of morphogenesis 2 (Daam2).

Daam proteins are a part of the formin family which play a role in the formation and elongation of actin microfilaments and microtubules. Dynein motors 'walk' along microtubules to transport cellular materials whilst ATMIN regulates DYNYLL 1. In light of the increase in Daam 2 protein where ATMIN is significantly reduced, it would be interesting to investigate if there is any communication between Daam proteins and ATMIN. The present project investigates whether ATMIN affects Daam2 and also cell growth.

Growth observations were made of human embryonic kidney cell line HEK293T before and after stimulation with Foxy 5 (Wnt5a agonist) or inhibition of ATM kinase inhibitor KU55933. When compared to its own vehicle control, the results seemed to reflect reduced cell growth and amplified ATMIN and Daam2 (n=3) for Foxy 5 treatments whilst KU55933 reflected increased cell proliferation and decreased ATMIN and Daam2 however the results were not statistically significant as no p value could be generated.

Equally, when the data was considered against both vehicle controls, a large variability in protein content was observed. Since the data lacked a significant p value and possessed a small sample size, the overall results proved statistically insignificant. The resulting conclusion was that there is more to explore in the possible ATMIN/Daam2 relationship.

Acknowledgements

I'd like to acknowledge the names of those who, through this project, have helped me,

Additionally, please allow me to describe this experience in poetry.

Embarking on this Masters by Research in Genetics degree,

Was an experience that will solidify itself in my memory.

Many challenges arose that allowed me the opportunity,

To develop my character, and test the boundary,

Test the boundary of my resilience,

All whilst gaining invaluable knowledge and experience.

There were times when I truly questioned myself,

Questioned the decision's I made, questioned the project itself!

With that said, embarking on this project was equally an opportunity,

To form bonds with colleagues and appreciate the people who continually supported me.

1st words of thanks goes to God almighty,

For sparing my life, guiding and directing me.

Next I'd like to say thank you:

To Dr. Paraskevi Goggolidou,

Who sparked my initial interest in the kidney,

And who encouraged me to pursue this degree.

To my parents especially my mother, Mrs. Barbara Pluck-King,

Who worked hard to provide consolation, money and anything lacking,

To Aunty Natasha and Uncle Denroy Lindsey,

Thank you for your support when I had nowhere to stay, you extended your home and heart to me,

To Aunty Terry Sithole, a lecturer at Kingston university,

And Chavelli Brewster, Olivia Riley, Ian and Lorraine Johnson, Morris Weekes and the rest of my church family,

I appreciate the listening ear and words of advice that you offered to me.

To Elizabeth Uhuka, my ride or die partner,

Thank you for your strength, encouragement and love like a sister.

To Miss Amtul Bhunnoo, I'm so happy to have met you as a laboratory partner,

We've been through this rocky journey together,

And formed a friendship bond so deep I hope it lasts forever.

To Mr. Promise Owhuo, an admirable man that made me desire to emulate his work ethics,

I love you and thank you for the example you set and your words of wisdom that gave me strength to continue in academics.

To Dr. Natasha Hill, thank you for your willingness to help and genuine concern

When I felt disadvantaged, you showed me lessons I could learn.

I'd like to say a massive teary-eyed thank you,

To the teacher that has impacted my life the most, Dr. Mark Carew,

You took up the challenge when I suddenly became your student,

Without complaint, you searched and provided a way out of this predicament.

You were a counsellor, encourager, a motivator, an editor,

Nit picking my work, pushing me to do better ☺

You always made time for me in your busy schedule and believed in me all the way through,

The completion of this project would not be possible without you.

Last but not least, Thank you to Almighty God, my heavenly Father,

Who reminded me that everything has its season and just like this project and its difficulties, won't last forever.

It's time for me to build on what I've learnt and move forward to the future!

1.0 INTRODUCTION

1.1 Rationale

Planar Cell Polarity (PCP) plays an important role in organ development and tissue morphogenesis (Butler & Wallingford, 2017). The ATM-INteracting protein ATMIN (ATM-substrate Chk2 interacting Zn^{2+} finger protein, ASCIZ) has emerged as a major contributor in the Wnt PCP pathway. Multiple roles for ATMIN have been discovered including its role in check-point signalling where it responds to single and double strand DNA breaks (Heierhorst, 2008). Cell check point signalling detects damaged or irregular DNA and coordinates cell cycle progression by slowing or arresting cell progression to allow time to repair and correct genetic lesions before they are inherited by the next generation of daughter cells (Abraham, 2001).

Additionally, ATMIN is involved in auto-regulation of DYNLL1. ATMIN activates DYNLL1 gene expression by binding directly to the promoter region of DYNLL1 and regulating its activity in a Zn^{2+} finger-dependent manner. This causes DYNLL1 protein to interact with ten binding sites in the ATMIN transcription activation domain (Figure 1). ATMIN therefore senses free DYNLL1 protein and high DYNLL1 levels inhibit

ATMIN transcription. This feedback loop enables regulation of DYNLL1 to meet cell requirements (Jurado, et al., 2011). This ATMIN-DYNLL1 feedback loop highlights the role of ATMIN in morphogenesis as it is required for normal lung morphogenesis and ciliogenesis (Goggolidou et al., 2014).

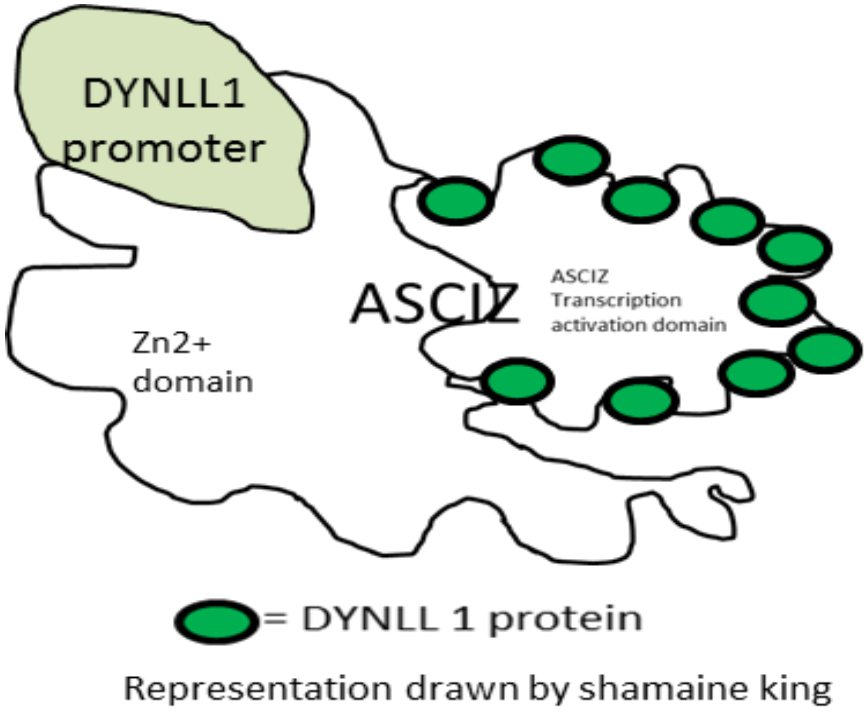

Figure 1 shows ATMIN (ASCIZ) binding directly to the promoter region of DYNLL1 in a Zn^{2+} dependent manner causing production of DYNLL1 protein which when free, binds to ATMIN at ten sites in its transcriptional domain resulting in ATMIN transcription inhibition.

Recently, ATMIN has emerged as a major contributor in the Wnt PCP pathway where it was shown to mediate kidney morphogenesis (Goggolidou, et al., 2014). ATMIN-deficient kidneys termed ATMIN Gasping6 kidneys have a point mutation in the ATMIN domain where cysteine substitutes serine. These kidneys displayed random oriented cell division (OCD), reduced length: width ratio and also perturbed cytoskeleton consistent with defective PCP (Goggolidou et al., 2014). Precise downstream cascade mechanisms by core PCP proteins are yet to be defined however, these apparently involve small GTPases of the RhoA family and Daam proteins (Tanegashima, Zhao & Dawid, 2008).Tissues known to require Wnt signalling express Daam proteins and they are also effectors of Wnt signalling during vertebrate development (Nakaya, et al., 2004).

This is interesting because protein expression levels measured in ATMIN Gasping6 kidneys included a two-fold upregulation of the Dishevelled associated activator of morphogenesis 2 (Daam2) protein (however Daam 1 level was unaffected).

The major question posed in this project is: could the morphogenesis mediator ATMIN, which is involved in the PCP Pathway, somehow interact with Daam2 in the same pathway with consequent effects on cell growth?

It was worthwhile investigating this question as it may hold key answers that provide insight into the mechanisms that link PCP to organ morphology and subsequently to morphological diseases.

1.2 Background

Nineteen eighty two saw the discovery of the first Wnt gene, mouse integration 1 (int-1), which was activated in the breast tumours of mammary tumour virus (MMTV) infected mice (Dudley, Golovkina & Ross, 2016). This gene was later renamed to Wnt-1 when the Wingless (Wg) gene affecting wing development in Drosophila melanogaster was identified as its homologue and so the Wnt signaling pathway derived its name from a portmanteau of Int and Wg (wingless) (Klaus & Birchmeier, 2008).

Wingless gene mutations in fruit flies were identified in wingless flies, whilst copies of the MMTV virus were found integrated into the mouse genome which forced overproduction of several Wnt genes and resulted in MMTV tumours. In an effort to comprehend how analogous genes yielded such diverse effects, current research has highlighted the importance of Wnt proteins, now classed as a major group of secreted morphogenic ligands, in pattern development establishment in multicellular organisms.

Wnts are a large family of highly conserved, secreted cysteine rich glycoproteins that cause cellular response by initiating cascades through three distinctive pathways (Figure 2). However, this is not to say that only specific Wnts activate specific pathways. The signaling mechanism is more complicated as previous Wnt ligands have been proven to activate both canonical and non-canonical pathways (Cha, et al., 2008). Additionally, the receptor context the Wnt interacts with plays a large role in pathway signalling because Wnts may also work together to activate pathways (Mikels & Nusse, 2006).

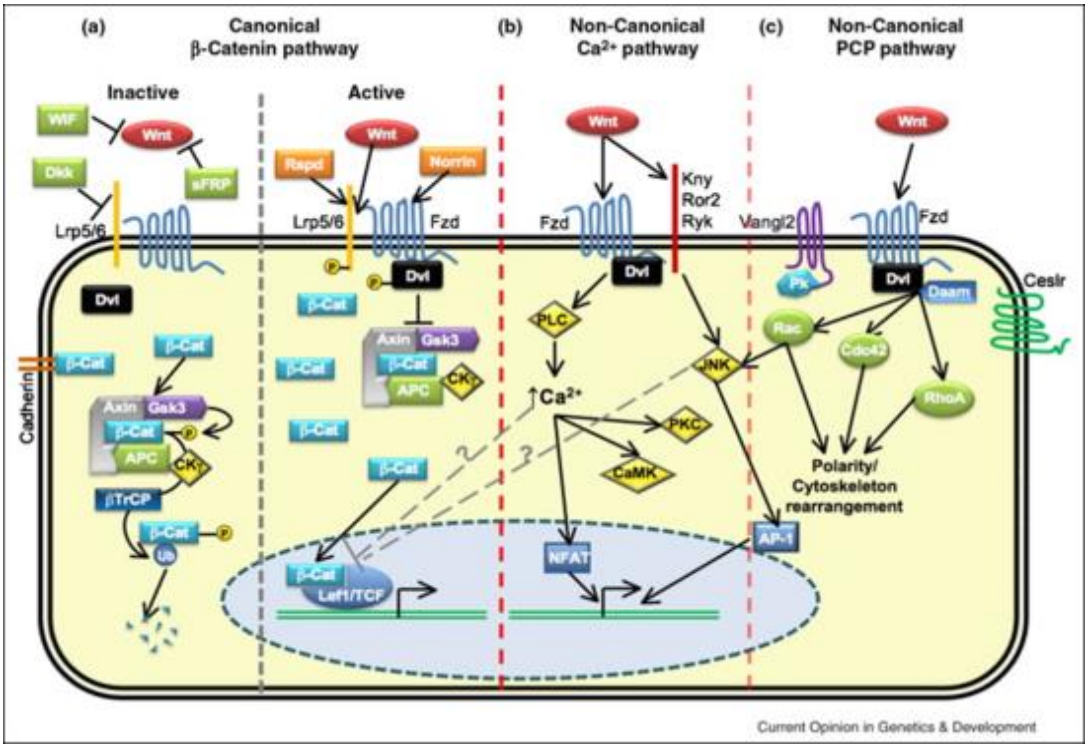

Figure 2 Shows the three known Wnt signalling pathways; The Canonical β-catenin dependent Pathway, Non-Canonical Planar Cell Polarity Pathway and the Non-Canonical Calcium mediated pathway.

From: Franco et al. Current Opinion in Genetics & Development 2009, 19:476–483

The β- catenin dependent or the 'canonical pathway' is the best understood pathway and normally results in cell proliferation and differentiation (Yang, 2012). In the absence of Wnt signaling, cytoplasmic β-catenin protein is prevented from reaching the nucleus as it is constantly degraded by Glycogen synthase kinase-3 (GSK-3), axin (a scaffolding protein), the tumor suppressor adenomatous polyposis coli (APC) and casein kinase 1 (CK1). These form a destruction complex that phosphorylates β-catenin, causing ubiquitination and subsequent proteasome degradation (MacDonald, Tamai & He, 2009). However, when canonical Wnt ligands bind to a frizzled receptor in the presence of lipoprotein receptor-related protein 5/6 (LRP 5/6), LRP5/6 is phosphorylated and Dishevelled (Dvl) is activated. Dvl inactivates or disassembles the destruction complex thus preventing β-catenin phosphorylation and effectively rescuing β-catenin from degradation. β-catenin is then able to reach the nucleus and regulate downstream gene expression (Yang, 2012).

Any other biological outcomes of Wnt signaling are termed non-canonical. Wnts can non-canonically regulate intracellular calcium mobilization but the functional significance of this in mammalian development is unclear. Intracellular calcium [Ca^{2+}] regulates the nuclear envelope passage that blocks the entry of large proteins. As β-catenin needs to cross this envelope to enter the mammalian

nucleus, Thrasivoulou, Millar & Ahmed, (2013), used live assay experiments using calcium dyes in PC3 prostate cancer cells to investigate which Wnts would cause calcium mobilization. They suggested that Wnt/Ca^{2+} and Wnt/β-catenin pathways acted in a synchronized manner and that [Ca^{2+}] release facilitates β-catenin entry into the nucleus in mammalian cells.

The third known Wnt signaling pathway is the non-canonical Planar Cell Polarity (PCP) pathway. PCP results in cytoskeleton rearrangement. It establishes cellular direction in a 2D epithelial plane of a tissue so that cells can differentiate the side of one cell from the side of another. This direction is established by directing the polarised alignment of cells perpendicular to the apical-basal axis (Anon, 2017b). This allows the cell to know which way is ‘up’ and is essential as most cells would fail to function without direction. For instance, microtubule based organelles called cilia align their basal bodies so that the polarized displacement results in cilia toward one cell edge (Wallingford, 2017). This localization to a specific side can potentially trigger a cascade of events such as coordinated directional beating (Figure 3). The directional beating of cilia is important for the movement of fluid during processes such as left-right axis patterning (Minegishi, et al., 2017) and kidney function (Goggolidou, et al., 2014b).

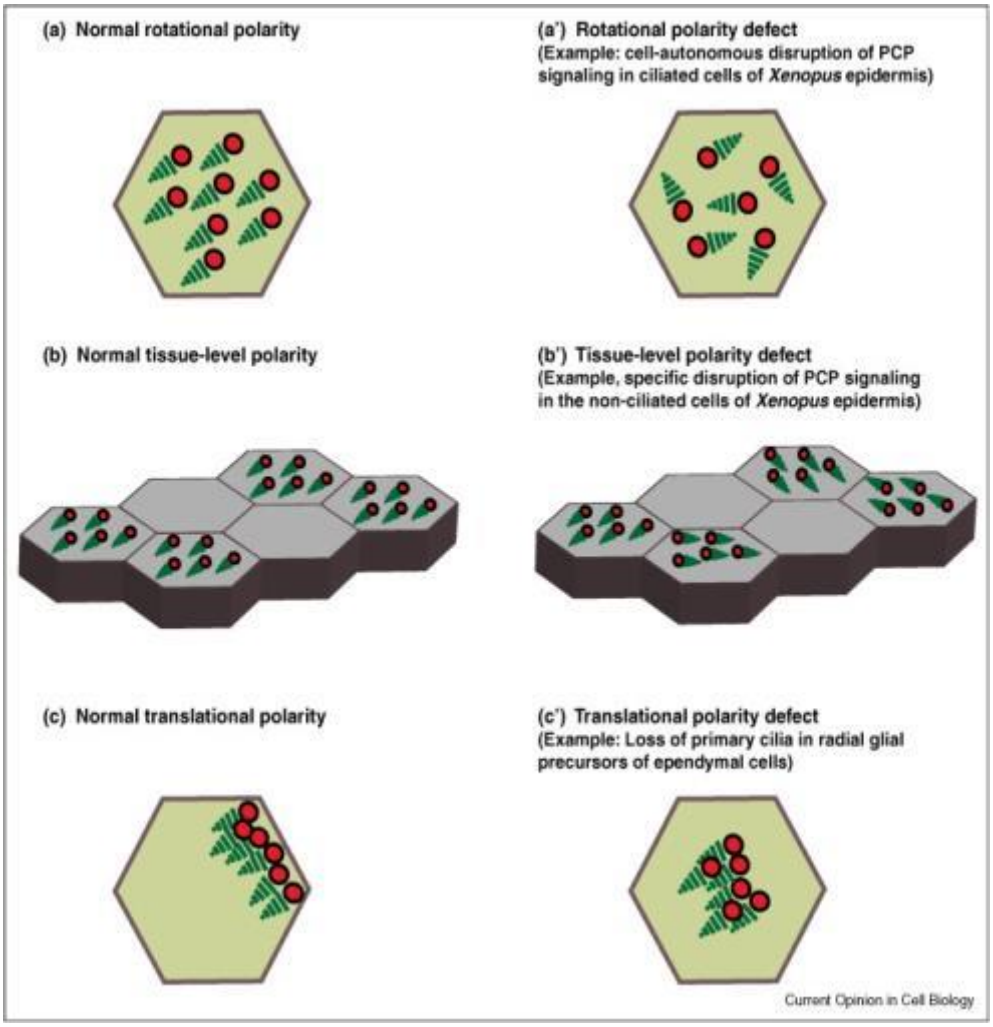

Figure 3 shows how multi-ciliated cells look during rotational, tissue level and translational Normal (a), (b), (c) and defective (a'), (b'),(c') planar cell polarity. Red represents the basal body whilst green is the rootlet of a multi-ciliated cell.

From: (Wallingford, 2017)

Similarly the orientation of epithelial cells will define the position of the apical lumen and therefore the collective tissue architecture demonstrating the importance of PCP in the formation of functional organs such as the kidneys (Goggolidou, 2013) and the lungs (Yates, et al., 2010). Modulation of the actin cytoskeleton causes asymmetric redistribution of core PCP proteins and results in essential contributions in: ciliary positioning (Song, et al., 2010), regulation of cell shape (Babayeva, Zilber and Torban, 2010), branching morphogenesis, directional cell movement, glomeruli maturation (Yates, et al., 2010) and also tubule elongation (Lienkamp, et al., 2012).

The importance of this pathway is highlighted by the many diseases seen when the pathway becomes defective. Pathway defects are consistent with abnormal kidney development and end stage renal Disease (Papakrivopoulou, et al., 2013) (Figure 4).

PCP also has implications in Polycystic Kidney Disease where tubules filled with fluid expand and disrupt normal kidney structure thus resulting in, end stage renal disease in the case of the more dominant form, Autosomal Dominant Polycystic Kidney Disease (ADPKD) (Luyten, et al., 2010) and death ranging from before birth through to adulthood in the rarer Autosomal Recessive Polycystic Kidney Disease (ARPKD) (Bremmer, 2010).

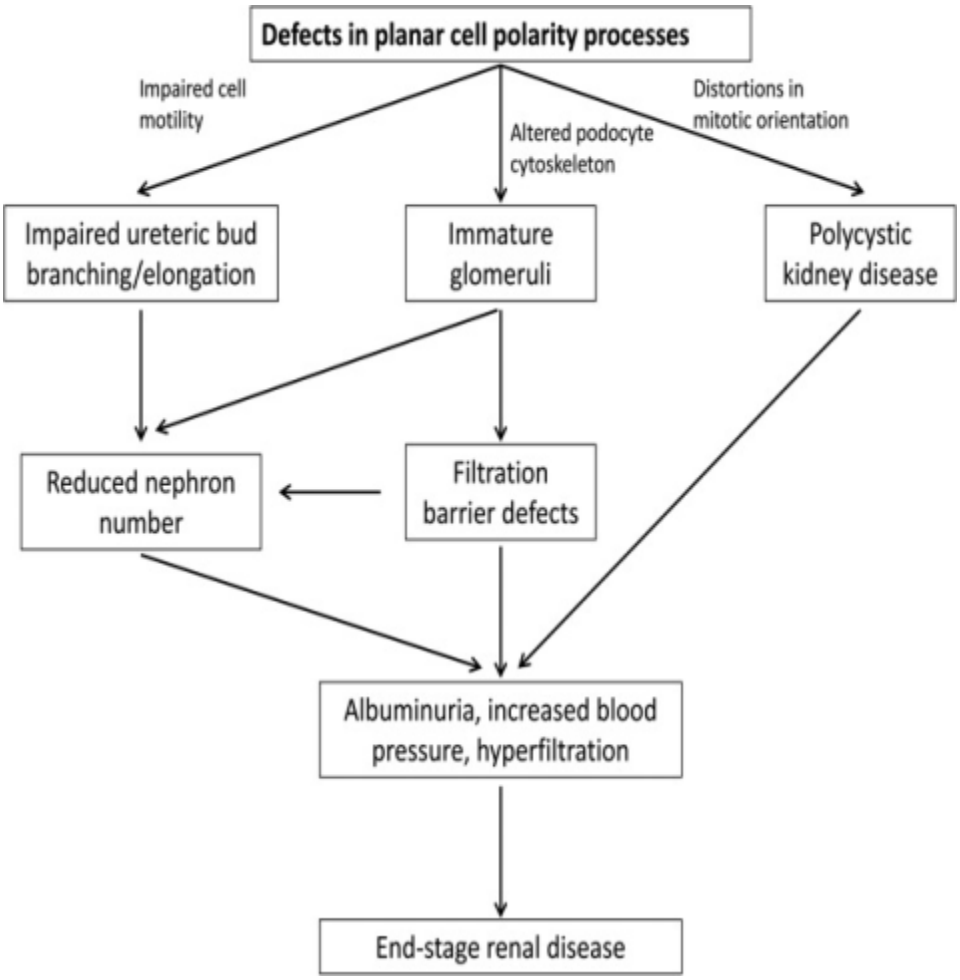

Figure 4 Defects in PCP processes lead to impaired branching and elongation of the ureteric bud, the formation of immature glomeruli and Polycystic kidney disease, all of which eventually lead to end-stage renal disease.

From : (Papakrivopoulou, et al., 2013)

As research increases, genes involved in the PCP pathway are becoming more defined. A number of molecular components implicating PCP genes with disease have been discovered. Examples identified include Vangl 2, Inversin, Wnt-9b, Fibrocystin, and ATMIN. Inversin, Fibrocystin, Vangl2 and ATMIN are shown in the PCP pathway in Figure 5. Dilated tubules, a mark of cyst formation, have been shown in Vangl2 mutants (Yates et al., 2010). Inversin deficiency resulted in nephronophthisis type 2 (a cystic kidney disease with reversed asymmetry) (Otto, et al., 2003) and loss of Wnt9b expression causes reduced rosette formations that are required for tubular elongation (Lienkamp et al., 2012). Fibrocystin is a membrane protein encoded by Polycystic Kidney and Hepatic Disease 1 (PKHD1) gene that is found in renal epithelial of cells and implicated in ARPKD (Patel, et al., 2008).

ATMIN has been shown to regulate both lung morphogenesis and ciliogenesis via DYNLL 1 (Goggolidou, et al., 2014b). Dynein is a motor protein (Rapali, P. et al., 2017). Motor proteins utilise ATP hydrolysis to drive muscle contraction and provide active transport of most proteins and vesicles in the cytoplasm by moving along the surface of a suitable substrate (Tocris Bioscience, 2017).

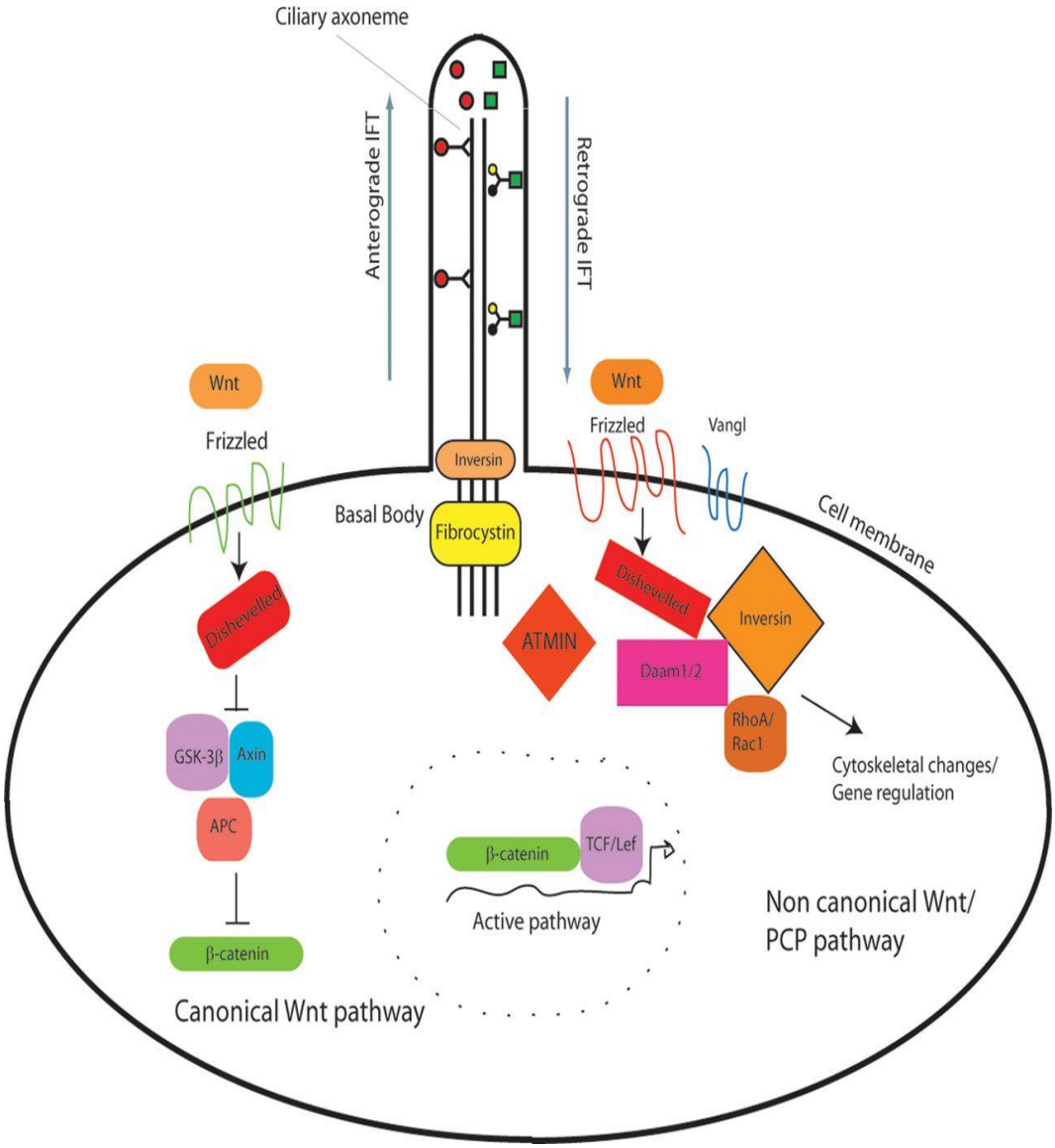

Figure 5 The canonical and non-canonical Wnt/PCP signalling pathways. The dashed line represents the nucleus where canonical Wnt signalling is activated thus resulting in transcriptional activation of downstream target genes. Fibrocystin and inversin localization to the cilium is also shown. ATMIN is represented by a red diamond. In this diagram, ATMIN could interact with either fibrocystin at the primary cilium or with Daam1/2 in the non-canonical Wnt/PCP Pathway.

From: (Goggolidou & Wilson, 2016)

Three superfamilies of cytoskeletal motor proteins exist. The Myosin motor superfamily acts upon actin filaments to direct cytoplasmic streaming, along with other morphological changes and vesicle motility. Additionally, it generates cell surface and muscle cell contractions. The kinesin and dynein microtubule based motor superfamilies move vesicles and organelles within cells, cause the beating of flagella and cilia, and act within the mitotic and meiotic spindles to segregate replicated chromosomes (Tocris Bioscience, 2017).

Dynein light chain 1 (DYNLL1, also known as LC8) was recognised as an associated light chain of dynein motor complex. It is required for proper folding and dimerization of the cargo-binding dynein intermediate chain (Rapali, P. et al., 2017). ATMIN binds directly to the promoter region of DYNLL 1 and regulates its activity in a Zn^{2+} finger-dependent manner to cause changes in ciliogenesis and morphogenesis though; specific molecular mechanisms are yet to be defined (Jurado, et al., 2011).

Additionally, ATMIN was seen modulating the Wnt pathway to control kidney morphogenesis (Goggolidou, et al., 2014a). Generation of the *Atmin*$^{gpg6/gpg6}$ mutant mouse that has a point mutation in cysteine to serine substitution resulted in embryonic lethality at mid-gestation. Reduced amount of renal vesicles and ureteric bud tips along with mis-

oriented cell division were apparent. When protein expression was measured in embryonic week 13.5 *Atmin*$^{gpg6/gpg6}$ mouse kidneys, mRNA expression of Wnt9b, Wnt11 and Dvl1 was decreased but Daam2 expression had increased. (Goggolidou, et al., 2014).

Dishevelled associated activator of morphology (Daam) is from the formin family and exists in two isoforms; Daam1 and Daam2. Daam1 is implicated in PCP signalling during *Xenopus* gastrulation and is necessary for convergent extension (which is PCP influenced) in *Xenopus* embryos (Habas, Kato and He, *2001*). According to the GenitoUrinary Development Molecular Anatomy Project (GUDMAP) Daam2 participates in determination of left/right symmetry, actin cytoskeleton organization and cellular component organization and its functions include actin binding and Rho GTPase binding. Daam2 is required for dorsal patterning via interaction and stabilization of Dvl 3/axin complex to pattern the developing spinal cord (Lee & Deneen, 2012).

As mentioned previously, PCP signalling results in cytoskeleton rearrangement. The cell cytoskeleton is made up of differing filaments; microfilaments, Intermediate filaments and microtubules. These filaments form to provide tensile strength and provide stability to the cell. Additionally they have roles in cell motility and transport of cellular material (Tocris Bioscience, 2017). Microfilaments are made up of

Actin. Individual Actin molecules termed G Actin (Globular Actin) come together in a nucleation process to polymerize and form F Actin (Filamentious Actin) (von der Ecken et al., 2014). Formin proteins such as Daam help determine where these filaments will form. This is because the FH2 domain in Daam proteins binds directly to both G and F actin respectively and have been shown to nucleate and elongate actin microfilaments (Kühn, S. and Geyer, M, 2014).

DAAM binds to F-actin and additionally to microtubules as it possesses the ability to crosslink the two filament systems. Accordingly, DAAM associates with the neuronal cytoskeleton, and a significant fraction of DAAM accumulates at places where the actin filaments overlap with that of microtubules (Szikora et al., 2017). Biochemical and cellular assays from Szikora et al., (2017) revealed that loss of *DAAM* affects the growth and morphology of microtubules. Hence this data suggests that in addition to being an actin assembly factor, DAAM is also involved in the linkage of filopodial actin remodeling to microtubule stabilization during axonal growth (Szikora et al., 2017).

Daam proteins are involved in the formation and stabilization of Actin microfilaments and microtubules whilst ATMIN regulates DYNLL 1 that is a part of the Dynein motor complex that walks on these

microtubules. Could there be possible communication between ATMIN and Daam?

1.3 Aim and Hypothesis

This project aimed to investigate the possibility of intracellular communication between ATMIN and Daam1/2 with consequent effects on cell growth and morphology.

To investigate this possibility in the absence of genetically modified samples, for example those produced from a siRNA knockdown approach, and in order to complete the work within a three month timespan (because of operational issues encountered during the project as described later) a pharmacological approach was adopted.

Growth observations were made of human embryonic kidney cell line HEK293T before and after stimulation with a Wnt receptor agonist (Foxy 5) or an ATM kinase inhibitor KU55933. There are no Daam1/2 inhibitors. However, HEK293 were shown to express ATMIN and ATMIN interacts with ATM kinase (Kanu, et al., 2015).

ATMIN is thought to mediate kidney morphogenesis and ciliogenesis separate to its involvement in DNA damage. In an experiment to test if ATMIN carried out its regulation independent of its DNA damage role, Goggolidou, et al. (2014b) analysed the intracellular localisation

of the DNA damage marker 53BP1 in wild-type and mutant Atmingpg6/gpg6 embryos. Accepted Genome instability would be indicated by relocalisation of 53BP1 into discrete nuclear foci (Schultz et al., 2000; Wang et al., 2002). This relocation was detected in wild-type embryos treated with an alkylating DNA damaging agent but not in mutant embryos. Though this evidence suggests an independent role, further experiments should be done to completely rule out the possibility of the involvement of DNA damage relating proteins. So far, any involvement of ATM kinase in Wnt PCP signalling has not been documented but it isn't excluded from theory because it has not been investigated.

In this novel hypothesis, the assumption is made that the ATM kinase inhibitor KU55933 may possibly disrupt any ATM kinase/ATMIN/Daam1/2 communication, with a possible effect on Daam1/2 protein levels.

Foxy 5 is a Wnt 5a mimicking peptide (Safholm, 2005). Daam1 activation was also induced by Wnt5a in MDA-MB-231 human breast cancer cell monolayers (Zhu, et al., 2012). Daam2 was suggested to modulate formation and stabilization of Wnt/receptor complexes in chick (Lee & Deneen, 2012). If Daam2 interacts with ATMIN, then Wnt5a activation may modulate ATMIN protein levels via the Daam2 upregulation.

The experimental hypothesis is that stimulation of HEK 293T cells with Foxy 5 (a Wnt agonist) will change the intracellular levels of both ATMIN and Daam 2 because of a previously unknown intracellular interaction between the proteins. Inhibition of ATM kinase (KU55933) will also perturb ATMIN and Daam2 levels because of a previously unknown molecular interaction between the two proteins. The alternative Null hypothesis is that Foxy 5 or KU55933 will only affect ATMIN, but not Daam2 levels, because no intracellular interaction between the proteins actually exists.

This hypothesis was tested by measuring changes in ATMIN and Daam2 protein expression in HEK 293T cells via western blot quantification. HEK 293T cell growth and confluence was recorded using an Incucyte Live Imaging Station, after treatment of HEK 293T cells with KU55933 (ATM kinase inhibitor), Foxy 5 (Wnt agonist) and their controls, dimethyl sulfoxide (DMSO) and sterile Phosphate Buffer Solution (PBS) respectively.

2.0 Materials and Methods

All cell culture, cell lysate and tissue lysate preparation was performed by the author of this thesis including all techniques described in the protocol below unless otherwise stated.

2.1 Tissue Immunofluorescence

Wild Type (Wt) and Heterozygous (Het) ENU-derived ATMIN Gasping 6 four month old mouse kidney sections were received from MRC Harwell in collaboration with Dr. Charlotte Dean (from National Heart and Lung Institute (NHLI), Imperial College). Kidneys arrived for use embedded in wax sectioned at 5µm. Sections were deparaffinised in Histochoice clearing agent (Sigma Aldrich) for 3 times 5 minutes and rehydrated in PBS (Sigma, 1 tablet in 100ml distilled water) for 10 minutes. To access intracellular antigens, detergent permeabilisation occurred using 0.1% Triton X-100 (Fisher Bio-Reagents) in PBS for 10 minutes. Non-specific binding sites were blocked with blocking serum (20% goat serum +0.5%BSA (Sigma Aldrich) in PBS) for 45 minutes and washed five times for 5 minutes with PBB (0.5% BSA in PBS). A wax pen (Sigma Aldrich 5mm tip) outlined a circle around each kidney, forming a liquid resistant boundary to keep the antibody within a specialised area. Sections incubated overnight at 4ºC in an artificially

humid environment (on wet paper towel within the slide box) with 100µl of Primary antibody. Primary antibodies (raised in rabbit): Polyclonal Daam1 (1:200), Polyclonal Daam2 (1:200, Thermofisher Scientific Invitrogen Catalog#: PA5-62373). Three times 5 minute PBB washes was performed the following day and incubated in secondary antibody for 1 hour. Secondary antibody (raised in goat): rabbit anti-Goat IgG (H+L) Superclonal™ Secondary Antibody, Alexa Fluor 555 (1:10,000, Thermofisher Scientific, Catalog#: A27017)

Afterwards, 3 times 5 minute washes in PBB was repeated and one PBS wash to remove the BSA. Slowfade Gold antifade mountant with DAPI (S36938 Invitrogen, 1:50) aided visualisation of cell nuclei.

Negative controls were processed identically with the exception that blocking solution substituted primary antibodies. Antigen-antibody interaction was visualized via fluorescence detection and performed at Imperial College, London (fluorescence microscope with mercury arc lamp).

2.2 Tissue Lysate Preparation

Wild Type (Wt) and Heterozygous (Het) ENU-derived ATMIN Gasping 6 four month old mouse whole kidney tissue samples were retrieved from a -80ºC freezer and transferred to an icebox. Clean work surface and handling was maintained with 70% IMS spray (Industrial Methylated Spirit, denatured ethanol, VWR Chemicals, Product# 23684.360). Tissue was cut quickly using a clean sharp scalpel to prevent degradation. A ratio of 10µl:1ml of protease and phosphatase inhibitor (Sigma Aldrich, Product# 1002274973) to Ripa Buffer (Thermofisher Scientific, Product# 89900) respectively was used. Therefore 500µl inhibitor and 5ml Ripa Buffer per sample was aliquoted. A magnetic ball added to the sample aided homogenization in the tissue lyser (Tissue lyser LT from Qiagen) set at 30 oscillations for 3 minutes. Samples were then centrifuged at 4ºC at 10,000rpm for 20 minutes. Pellet was discarded and the magnetic bead was washed with Tween20 (Sigma Aldrich) whilst the supernatant was transferred to new Eppendorf tube. Samples were stored at -20ºC. One fifth of the sample (1100µl) was extracted and diluted with water (4400µl) in preparation for protein quantification.

2.3 Cell Lysate Preparation 2: 293T Human Embryonic Kidney (HEK) Cells

293T HEK Cells were chosen as they were used as controls for Daam 2 primary antibody (Thermofisher.com datasheet, 2017) and in an experiment where ATMIN was detected (Kanu et al., 2015). Although the author suggested that HEK cells while from the kidneys are closer to progenitor neuronal cells, the cells were still chosen because of availability and the project's short timeframe. These are epithelial adherent cells located in human embryonic kidneys derivative of human embryonic kidney 293 cells that contain SV40 T-antigen (Anon, 2017a)

293T (ATCC CRL-3216) cell culture protocol was used. Samples were thawed in water bath (37˚C) for 2 minutes then transferred to pre-incubated medium (1 bottle of Dulbecco's Modified Eagle's Medium (DMEM, 500ml, Sigma Aldrich, Product# D5796) +50 ml Foetal Bovine Serum (FBS, Sigma Aldrich, Product# F9665) no pen/strep) in a 25 cm^2 flask. Cultures were incubated at 37˚C taking 3 days to reach 70% confluency. Cells were received at passage number 15 as a kind gift from Dr.Chioni (Kingston University). To passage cells, they were removed from incubator and medium discarded. The cell layer was rinsed in 5 ml PBS (sterile, Phosphate Buffer solution without Ca^{2+},

Sigma Life Science, Product# D8662) solution and incubated for 5 minutes. 3 ml of Trypsin-EDTA solution (Sigma Aldrich) added and incubated for 3 minutes. 7 ml of media was added to stop trypsin reaction. 1ml of solution was added to a new pre-incubated T75 flask containing 20 ml of media. The culture vessel was placed in the incubator and passaged after attaining 70% confluency. Medium renewal occurred 2-3 times per week.

Cells were washed in 5 ml of PBS and lysed for 20 minutes on ice using 1 ml Ripa Buffer (Thermofisher Scientific, Product# 89900) and 10µl of protease inhibitor (Sigma Aldrich, Product# 1002274973). Sample centrifuged at 4˚C at 12,000 rpm for 20 minutes and supernatant transferred to an Eppendorf tube for subsequent protein quantification.

2.4 Inhibitor Application

ATM-kinase inhibitor KU55933 (Tocris,Catalogue# 3544) was used on cells at 10 µM for 1 hour resulting in downstream effects on other signalling proteins (Hickson, 2004). Foxy5 (Tocris, Catalogue# 5461) which is a Wnt 5a agonist that was used in a wound healing assay at 100 ng/ml(Zhang, et al., 2014). Hence calculations for KU55933 were done to dose cells with 10µM KU55933 whilst Foxy 5 was added at 100ng/ml.

Calculations:

KU55933 makes a stock of 10 mM in DMSO. It is soluble to 100 mM DMSO.

10 mg of KU55933 inhibitor (MW399.99) in 2.5 ml of DMSO = 10 mM

So 10 µl in 10 ml = 10 µM

Control is 1/1000 DMSO in culture medium e.g. 10 µl DMSO in 10 ml DMSO

Foxy 5 comes as a powder weighing 1 mg. Soluble to 1mg/ml in PBS (sterile). So just add 1 ml to sterile PBS. It is used at 100 ng/ml. Make a 1/10 dilution to 100 µg/ml in PBS equal to 10 µl in 10 ml.

Control is 10 µl PBS in culture medium.

HEK293T cells were cultured in T-75 flasks and 6 well plates; the latter were kept in the Incucyte machine to obtain cell growth data. Culture vessels from either the incubator or the Incucyte machine were removed after attaining 50% confluence. They were then washed with 3 ml PBS, treated with drugs for 1 hour and then washed with 3 ml of PBS. The culture medium was then replaced and the cells replaced in the incubator until full confluency was obtained in the controls. The 6 well plates were placed back in the Incucyte machine to continue collecting growth data.

In T-75 Flasks:

One flask was treated with KU55933 inhibitor (10 µM, 20 µl in 20 ml of DMEM media), and a second flask was treated with its control, dimethyl sulfoxide (DMSO, supplier VWR) (20µl in 20 ml of DMEM media). A third flask was treated with Foxy 5 (100ng/ml, 20µl in 20 ml of DMEM media) and a fourth flask was treated with its control, sterile PBS (20µl in 20 ml of DMEM media).

In 6 well plates:

In the first 6 well plate, the top three wells were treated with KU55933 inhibitor. KU55933 inhibitor 10 µM solution was made by adding 10 µl of inhibitor in 10 ml of DMEM media and then 3 ml of this solution was pipetted into each well. Additionally in the first 6 well plate, the bottom

three wells were treated with KU55933 control, DMSO. DMSO solution was made by adding 10 µl of DMSO in 10 ml of DMEM media and then 3 ml of this solution was pipetted into each well.

In the second 6 well plate, the top three wells were treated with Foxy 5. Foxy 5 100 ng/ml solution was made by adding 10 µl of inhibitor in 10 ml of DMEM media and then 3 ml of this solution was pipetted into each well. Also in the second 6 well plate, the bottom three wells were treated with Foxy 5 control, sterile PBS. PBS solution was made by adding 10 µl of PBS in 10 ml of DMEM media and then adding 3 ml of this solution into each well.

2.5 Protein Quantification

Protein quantification was performed using a Bicinchoninic Acid (BCA) Assay (Thermofisher Scientific). A chelate complex is formed when peptides bond with cupric (Cu^{2+}) ions in an alkaline medium (containing sodium potassium tartrate). Hence the protein reduces Cu^{2+} to Cu^{+} forming a light blue coloured complex in a reaction called the Biuret reaction. Two molecules of BCA then react with 1 molecule of Cu^{+} producing an intense purple-coloured reaction. The BCA/copper complex is water-soluble and as protein concentration increases so does linear absorbance at 562 nm (Pierce BCA Protein Assay Kit, 2017).

Bovine Serum Albumin (BSA) standards were diluted in distilled water giving the following concentrations: 2000, 1500, 1000, 750, 500, 250, 125, 25, 0 (µg/ml). 25µl of each standard and unknown was pipetted into a 96-well plate in 3 replicates. This provided the assay with a working range of 20-2000µg/ml.

The kit utilized two reagents, A and B. The working reagent was prepared by combining A with B in the ratio 50:1 respectively. Amount of working reagent needed was derived from the formula:

(#standards + #unknowns) x (#replicates) x (volume of WR per sample in ml)

200µl of the working reagent was added to each well and the plate placed on a shaker for 30 seconds. Incubation took place at 37ºC for 30minutes after which the plate was read at 562nm on an Infinite M200 Pro TECAN running Magellan software. An Excel spreadsheet was generated and the absorbance values were averaged. The blank was subtracted and a scatter graph was plotted based on those values. A linear line was fitted and the equation generated from the line was used to calculate protein concentration of unknown samples. Total protein concentration was calculated by multiplying this value by the protein dilution factor (1/5).

2.6 Co-Immunoprecipitation

Co- immunoprecipitation experiments were performed to capture and purify the primary target but also to identify any macromolecules that might interact with the target antigen. Using ATMIN Gasping 6 four month old mouse kidney tissue lysates, pools of nine Wt and nine Het samples were made respectively. Protein was quantified via BCA Assay. 1 mg of protein was added to a new Eppendorf tube. 1 µg of normal rabbit IgG (Cell Signalling) was added as a control measure to preclear the lysate thus minimising non-specific binding and improving background. This together with 20 µl of re-suspended Protein A/G

PLUS Agarose (Santa Cruz Technology) was incubated at 4˚C for 1 hour and then centrifuged at 2500 rpm for 5 minutes at 4˚C.

Ten microlitres of Primary antibody was added to every 1 ml of lysate needed and incubated at 4˚C for 2 hours. The sample was then incubated at 4˚C overnight on a roller with 20 µl of re-suspended Protein A/G PLUS-Agarose. Immunoprecipitates were collected by centrifugation at 2500 rpm for 5 minutes at 4˚C. The pellet was washed four times with 1 ml Ripa Buffer and repeated centrifugation step between washes. Forty microlitres of 1x Laemmli Buffer was added to each supernatant and they were kept to run as controls on an SDS-PAGE gel along with 10 µl of the original lysate. After the final wash, the pellet was re-suspended in 40 µl of 1x Laemmli sample buffer. The samples were boiled for 3 minutes at 95˚C and 20 µl aliquots were loaded on an SDS-PAGE Gel along with the controls and followed the Western Blotting Protocol outlined. Unused samples were stored at -20˚C.

Primary antibodies (Raised in rabbit): Polyclonal ATMIN (1:200, Millipore), Fibrocystin (1:200, Santa Cruz Biotechnology), Inversin (1:350, Invitrogen),

Loading control antibody (raised in mouse): HSP60 (1:1000, Abcam).

2.7 Western Blotting

The Western Blotting process consisted of running the protein on a gel via electrophoresis, transferring it onto a membrane, probing for target antigens and then visualising and analysing the protein detected. A List of all Western Blotting solutions and gel recipes is found in Appendix 1.

2.8 SDS-PAGE Gel Electrophoresis

A range of 20-100 µg of protein was loaded into 10 well, 20 µl capacity, hand-made 7.5% SDS-PAGE gels. To every 10 µl of sample lysate, 3 µl of 1x Laemmli sample buffer was added. Samples were heated at 95ºC on a heat block for 10 minutes and then cooled at room temperature for 10 minutes. To verify electrotransfer and determine molecular weights, 3 µl of Precision Plus Protein Standard (Bio-Rad) was used as a protein marker in early western blots but later 8 µl of SDS-Page Ruler Plus Prestained Protein Ladder (Thermofisher Scientific) was used due to cost effectivity. During gel electrophoresis, proteins separated by size after running at 20 mA for 20 minutes

(stacking gel) and 40 mA for 80 minutes (resolving gel).Ten times Running Buffer was made as stock and diluted to 1x as needed (100 ml of 10x Running Buffer plus 900mls of distilled water). One times Running Buffer (200 ml) filled the inner compartment of the gel and 400 ml filled the outer compartment to the indicated line.

The dimensions of the gel made were:

Gel size: 6.5L x 8.5W. Gel Thickness: 0.7mm and 1.5mm

2.9 Immunoblot (Transfer Process) 1: Wet Transfer

After electrophoresis, wet transfer buffer was used to equilibrate the gel for 10 minutes and pre-soak extra thick filter paper (14 x 16cm, Bio-Rad) and fibre pad. For correct transfer, gel sandwich was placed on the wet transfer cassette in the following manner: (grey side down) pre-wetted fibre pad, filter paper, gel, membrane, filter paper, pre wetted fibre pad. The cassette was closed and inserted into the chamber. The gel was electroblotted onto nitrocellulose membrane (0.2 µm pore size Amersham Protran) and ran at 12 V for 42 minutes.

2.10 Immunoblot (Transfer Process) 2:Semi-Dry Transfer

Following electrophoresis, semi-dry transfer buffer was used to equilibrate the gel for 5 minutes and pre-soak extra thick filter paper (14 x 16cm, Bio-Rad). For correct transfer, gel sandwich was placed on the Semi-Dry blotting machine in the following manner: Filter paper, membrane, gel, filter paper. A roller removed air bubbles. The gel was electroblotted onto PVDF membrane (0.2 µm pore size Amersham Protran) (pre-wetted in methanol to activate) and ran at 100 V for 1 hour. An ice pack was placed in the tank and the tank placed in a box of ice to prevent overheating.

2.11 Protein Visualisation

For qualitative visualization, post transfer, the membrane was stained with Ponceau (Sigma Aldrich) where bands stained red if they were transferred whilst the gel was stained with Coomasie blue (Sigma Aldrich) to check for bands that remained on the gel and were not transferred. This aided optimisation of transfer times resulting in efficient protein transfer. Washing in TBS/T removed Ponceau as it was a reversible stain. 5% milk (2g semi-skimmed milk, 40mls TBS/T) was used as blocking solution to block non-specific binding sites for 1

hour at room temperature. The blocking solution was decanted and replaced with the primary antibody of interest at varying dilutions in 10 ml of the blocking solution **(See table 1.0).** After incubating overnight at 4ºC the solution was decanted and washed 3 times for 5 minutes with 20 ml of TBS/T. The membrane was then incubated with secondary antibody diluted in 10 mls of blocking solution for 2 hours. The membrane washed again 3 times for 5 minutes in TBS/T and was placed onto the ODYSSEY Classic Version X machine to be scanned at wavelengths 700 nm and 800 nm.

The Western Blotting technique utilized two spectrally different Near-Infrared (NIR) labelled secondary antibodies to facilitate normalization of target proteins. Anti-rabbit secondary IRDye 800 CW (LICOR) appeared green on channel 800nm whilst Anti-mouse secondary IRDye 680RD (LICOR) appeared red on channel 700nm.

Table 1.0 Western Blotting Antibody information

	Host Species	Name	Dilution factor	Volume in 10mls Blocking Solution	Molecular weight (kDa)	Manufacturer	Catalogue Number
Primary Antibodies	Rabbit	Daam 1	1/500	20ul	130	Thermofisher, (Invitrogen)	PA5-23222
		Daam 2	1/500	20ul	130	Thermofisher, (Invitrogen)	PA5-14550
		Atmin	1/200	50ul	110,120	Millipore	Ab3271
		Atmin	1/200	50ul	110,120	Cambridge Bioscience	A303-399A-M
		Inversin	1/200	50ul	118	Abcam	ab65187
House keeping protein	Mouse	HSP60	1/1000	10ul	61	Abcam	ab89609
		Actin	1/1000	10ul	42	Thermofisher	PA1-183
Secondary Antibodies	Donkey	Anti-Rabbit	1/10000	1	N/A	LICOR	926-32213
		Anti-Mouse	1/10000	1	N/A	LICOR	926-68072

2.12 Quantification of Immunoblots

Blots were analysed from 23rd to 24th March 2017 relative to the loading control HSP60 in earlier blots and to β-actin in later blots using Image Studio Software for the ODYSSEY Classic Version X from LICOR. The membrane was placed on the scanner and settings set to 'Western' scan, with the intensity level set to 5 for both channels 700 nm and 800 nm. Western analysis was chosen on the analysis menu and each sample (labelled as L and a number) and marker lane (labelled M1) was designated by a line. The 'background' was set to 'lane'. This background calculation measures the intensity of the pixels in each lane and subtracts it from the band. Thus, when the same sized rectangle was placed around selected bands, signal values were applied based on that calculation which was equivalent to the amount of light emitted on that channel minus the background of that lane (Figure 6). The bands in the marker lane (M1) had set values that arrived with the selected marker ladder. For example, SDS-PAGE pre-stained marker has set sizes of 250kDa, 130kDa, 100kDa, 70kDa, 55kDa, 30kDa, 25kDa, 15kDa and 10kDa. The bands in the sample lanes were assigned size values using the marker band sizes as a reference.

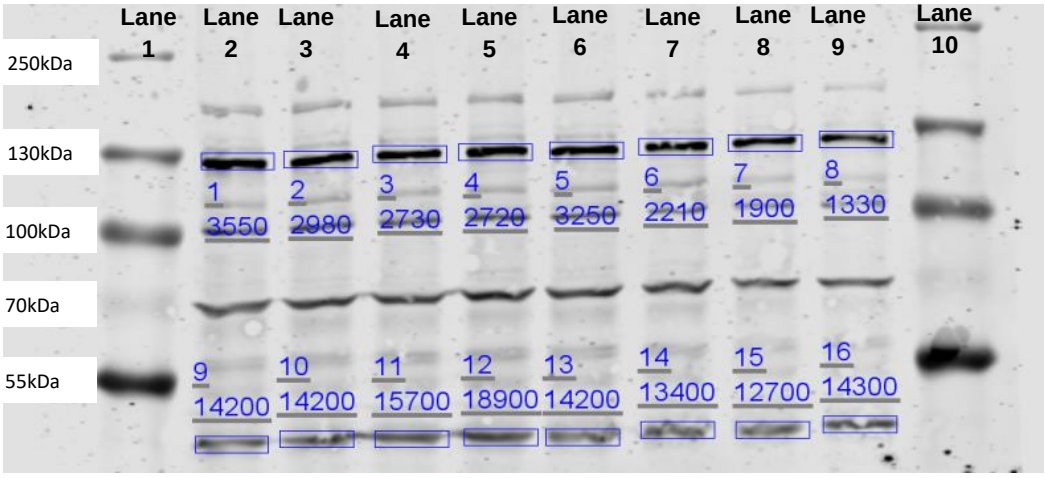

Figure 6 An example of a quantified blot where the same sized rectangle was copied and placed over each band. Lanes 2-8: normal HEK 293 lysates. Lanes 1, 10: marker lanes. The membrane was probed for Daam2.

Since the loading control was beta-actin which is detected on channel 700nm, that channel was selected to normalize the data. The band on that channel that possessed the largest signal was assigned a value of 1. The signals from each of the other bands were divided by the largest signal to obtain the normalization factor of the band in the same lane. The normalization signal was then found by dividing the Daam2 signal intensity by the normalization factor. The geometric mean (GM) of the normalized signal was calculated instead of the arithmetic mean because during normalization of data, the geometric mean was less affected by outliers so it compensated for very high and very low values.

3.0 Results

In an investigation into the molecular mechanism of ATM activation by replication stress, Kanu et al 2015 measured ATMIN expression in HEK 293T cells to show that ATMIN, WRN interacting protein 1 (WRNIP1) and RAD18, the E3 ligase responsible for PCNA monoubiquitination, specifically activated ATM signalling in response to replication stress and contributed to the maintenance of genomic stability. However, it should be noted that HEK 293 were derived from HEK293T cells. The SV40 large T antigen was used to transform HEK 293 cells and therefore possess significant divergence from HEK293 cells.

3.1 HEK 293T cells express ATMIN and DAAM 2 protein

In the present study, ATMIN expression via western blotting was found in normal HEK 293T cells after culturing and cell lysis (Figure 7). A secondary antibody with a fluorophore attached to it allowed for detection of ATMIN and its loading control, β-Actin. The ATMIN antibody was raised in rabbit and so an anti-rabbit secondary antibody with a green fluorophore was employed that fluoresced at 800nm. Alternatively, the β-actin antibody was raised in mouse and hence an

anti-mouse secondary antibody with a red fluorophore attached was utilized and detected at 700nm.

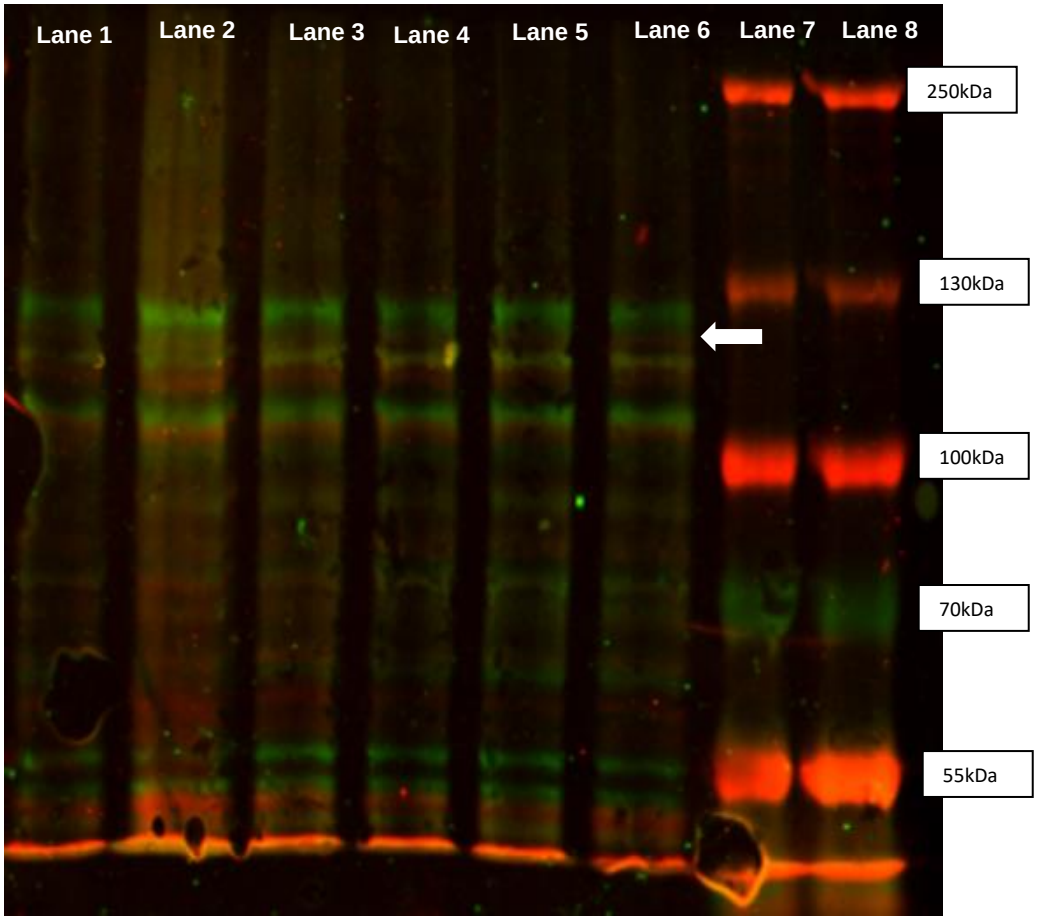

Figure 7 Lanes 1-6, lysates of unstimulated HEK 293T cells. 20µg of protein loaded. ATMIN was detected as expected at 110/120 kDa (white arrow)using primary antibody 1:200. Lanes 7-8: prestained markers. Multiple green bands present.

Subsequent western blot results also showed that HEK 293T cells expressed Daam2 (Figure 8). The Daam2 antibody was raised in rabbit and so an anti-rabbit secondary antibody with a green fluorophore detected at 800nm was used.

The marker lanes at both ends of the blot, aided identification of the target antigen. Markers had set band sizes and the Licor Image Studio software used this to estimate the size of the band to draw a rectangle around. Daam2 is approximately 130kDa and appeared at the estimated 130kDa band size. β-Actin is approximately 42kDa and appeared at that molecular weight.

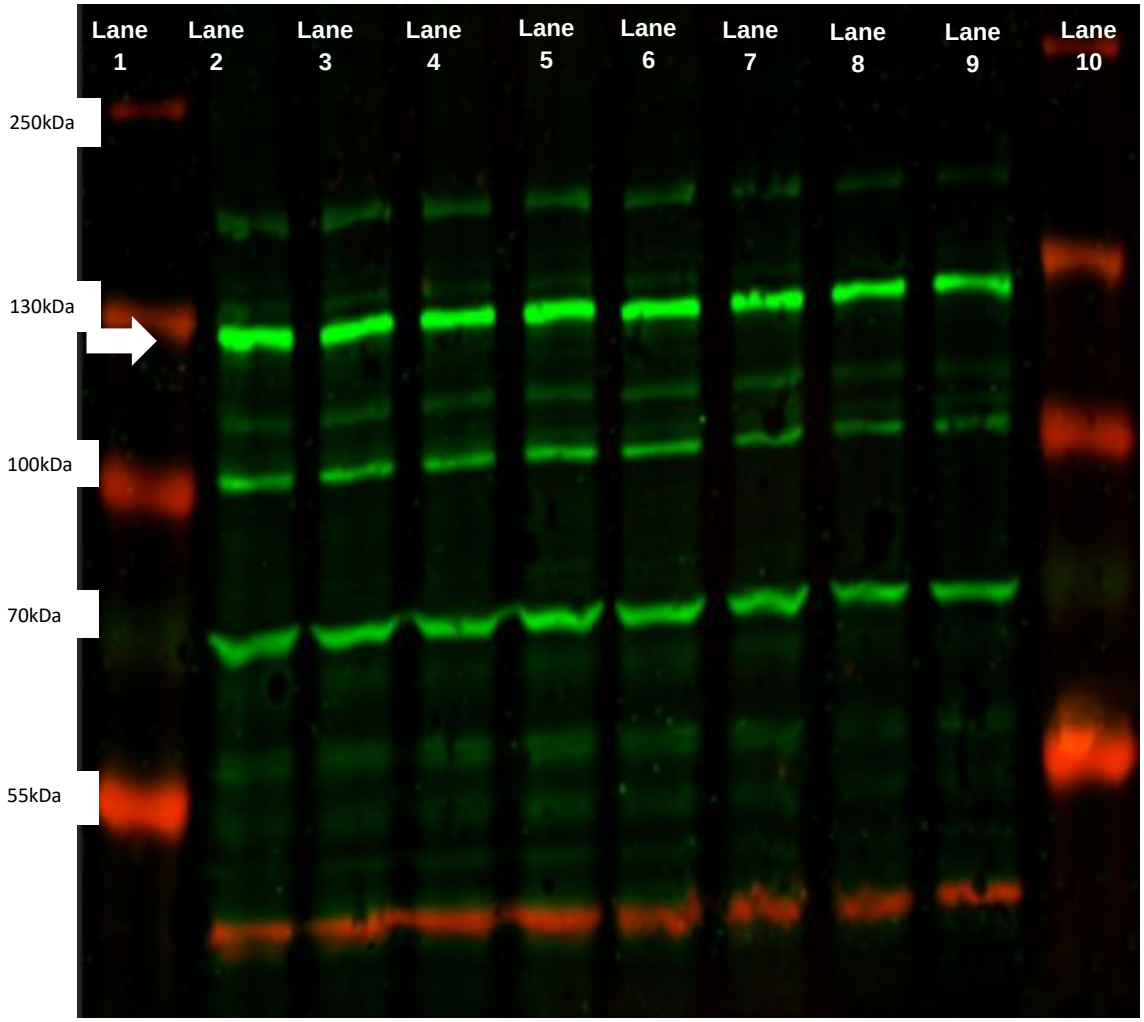

Figure 8 Lanes 2-9 Western blot of Daam2 protein in normal unstimulated HEK 293T lysates. Daam 2 was detected at 130 kDa (white arrow) although other bands were also detected. Primary antibody (1:200). Lanes 1 and 10 are marker lanes. Multiple green bands present.

There were multiple extra bands detected on the blots. According to Bio-rad.com (Western blot troubleshooting guide, 2017) multiple nonspecific bands on a western blot may occur for several reason. The primary or secondary antibody concentration may be too high or there may be cross-reactivity between either the primary or secondary antibody with the blocking agent or with similar epitopes on other proteins.

To verify if the secondary antibodies bound non-specifically, a control experiment was performed with all sample lysate types on the membrane without the addition of primary antibody. The membrane was simply blocked and the secondary antibody applied for the same two hour period as usual. Figure 9 showed no signal meaning the secondary antibodies were not the problem.

Additional explanations for this problem include a low purification of the antibody used such that it recognised additional complexes. The extra bands may therefore be ATMIN or Daam2 like fragments detected by the primary antibodies. The purchased Daam2 antibody was purified via affinity chromatography whilst ATMIN was also affinity purified.

A future direction for this type of project would be to improve the western blotting protocol. The western blotting method normally needs to be adjusted to each antibody that is being used. For instance, the

antibody concentration may be too high or some blots may require longer blocking times or washing periods thus more experimental conditions and antibody titration would result in better blots and less background.

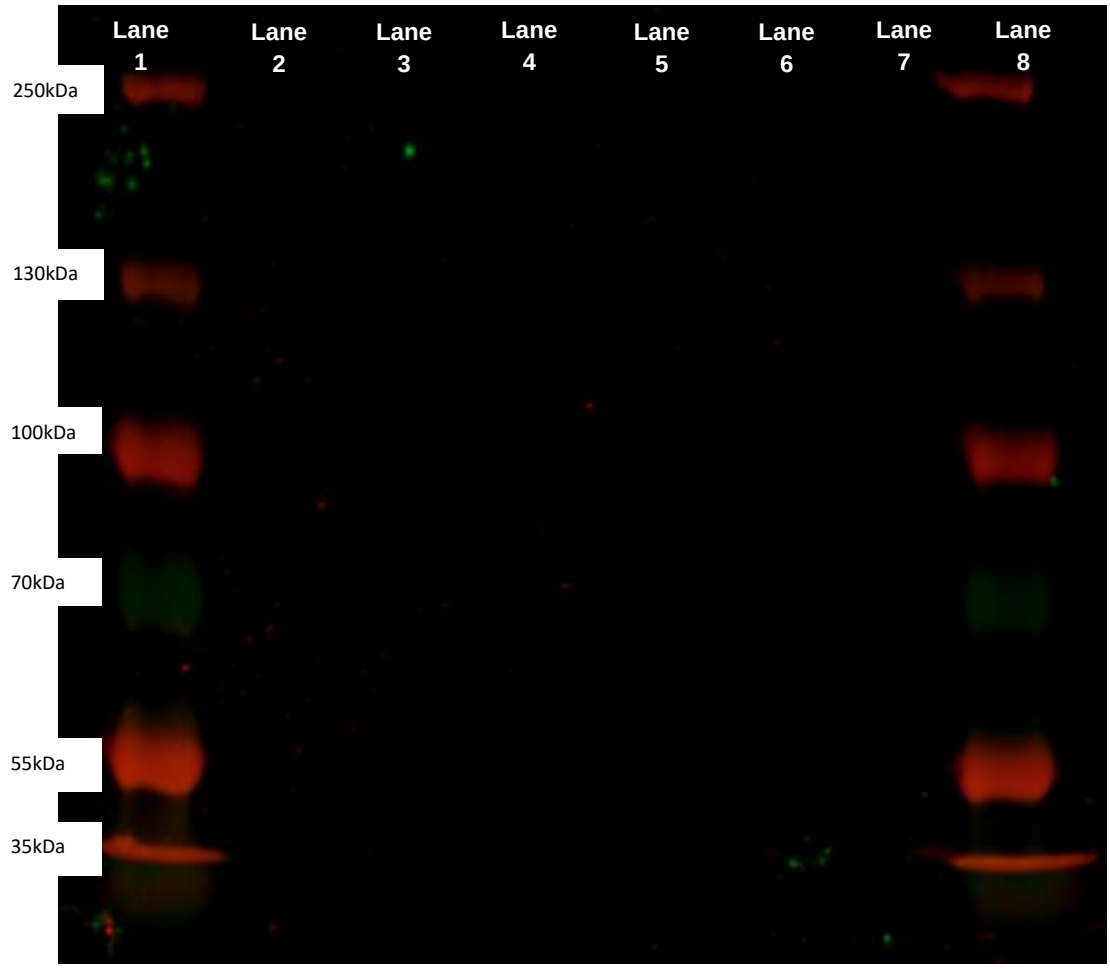

Figure 9 Lane 2 - KU55933 inhibitor, Lane 3 - KU55933 control, Lane 4 - Foxy 5 inhibitor, Lane 5 - Foxy 5 control, Lane 6 – unstimulated HEK293 lysates, Lane 7 - unstimulated HEK293 lysates. The primary antibody was omitted. The secondary antibody (1:10, 000 dilution) was added. Otherwise the protocol was the same. Lanes 1 and 8 are markers.

3.2 Effect of ATM kinase inhibitor KU55933 on ATMIN and Daam2 expression in HEK293T cells

HEK293T cells were cultured in 6 well plate culture vessels until half confluency was attained. KU55933 was added at a final concentration of 10μM for 1 hour to the top three wells. The drug vehicle (DMSO 0.1%) was added to the bottom 3wells. Medium was replaced and the plates were incubated until the control cells reach confluence, after which cellular lysates were prepared and stored at -20˚C for western blots.

Tables 2.0 and 3.0 respectively show the calculated normalized signal of ATMIN and Daam2 in 6 well plates relative to β- actin in experiments 1 and 2. The 'Raw Data' columns show the quantified signal detected by the Image Studios Western blot software. The normalization factor was generated by dividing all the β-actin values on the 700nm channel by the largest β-actin value. The normalized value then resulted from the original signal divided by the calculated normalization factor for that lane.

		Experiment 1							
		ATMIN				Daam 2			
	Loading Lane Number	KU55933 control	KU55933 inhibitor	Foxy 5 control	Foxy 5 inhibitor	KU55933 control	KU55933 inhibitor	Foxy 5 control	Foxy 5 inhibitor
Raw Data	800nm Channel Integrated Intensity (I.I) Signal of ATMIN	15.231	19.373	19.833	19.506	4.002	1.27280561	0.157	2.375
	700nm Channel Integrated Intensity (I.I) Signal of Beta-Actin	16.491	30.607	29.731	26.259	123.942	345.34375	185.472	230.555
Normalized Data	Relative Beta-Actin I.I Signal (normalization factor)= All Beta-Actin I.I signal/greatest Beta-Actin I.I signal	0.539	1.000	0.971	0.858	0.359	1.000	0.537	0.668
	Adjusted Values = ATMIN signal I.I / relative Beta-Actin I.I signal (normalization factor for that lane	28.272	19.375	20.419	22.738	11.150	1.273	0.292	3.558

Table 2.0 Normalized signal of ATMIN and Daam2 relative to β-actin when treated with the ATM-kinase inhibitor KU55933, its vehicle control (DMSO) and

		Experiment 2							
		ATMIN				Daam 2			
	Loading Lane Number	KU55933 control	KU55933 inhibitor	Foxy 5 control	Foxy 5 inhibitor	KU55933 control	KU55933 inhibitor	Foxy 5 control	Foxy 5 inhibitor
Raw Data	800nm Channel Integrated Intensity (I.I) Signal of ATMIN	1.287	1.535	1.995	2.642	7.196	12.584	14.196	5.188
	700nm Channel Integrated Intensity (I.I) Signal of Beta-Actin	29.660	29.129	44.000	23.520	60.605	132.637	105.672	77.335
Normalized Data	Relative Beta-Actin I.I Signal (normalization factor)= All Beta-Actin I.I signal/greatest Beta-Actin I.I signal	1.018	1.000	1.510	0.807	0.457	1.000	0.797	0.5830
	Adjusted Values = ATMIN signal I.I / relative Beta-Actin I.I signal (normalization factor for that lane	1.264	1.535	1.321	3.273	15.749	12.584	17.818	8.899

Table 3.0 Normalized signal of ATMIN and Daam2 relative to β-actin when treated with the ATM-kinase inhibitor KU55933, its vehicle control (DMSO) and Foxy 5 and its vehicle control (PBS) in 6 well plate experiment 2.

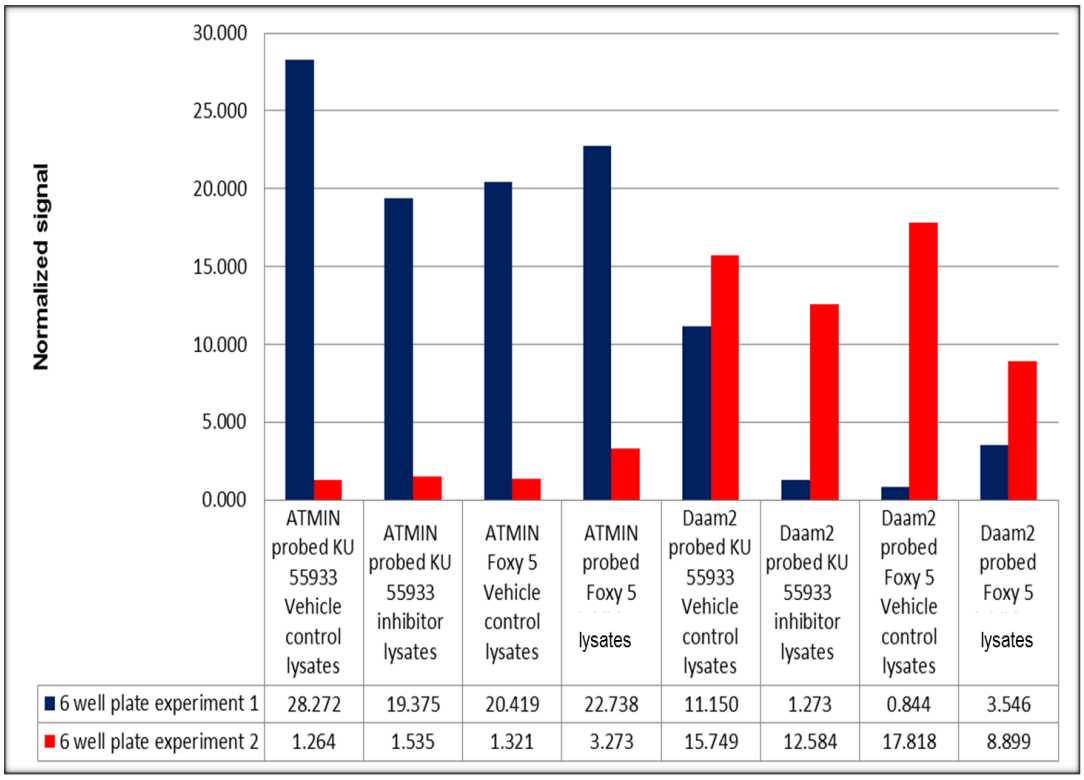

	ATMIN probed KU 55933 Vehicle control lysates	ATMIN probed KU 55933 inhibitor lysates	ATMIN Foxy 5 Vehicle control lysates	ATMIN probed Foxy 5 lysates	Daam2 probed KU 55933 Vehicle control lysates	Daam2 probed KU 55933 inhibitor lysates	Daam2 probed Foxy 5 Vehicle control lysates	Daam2 probed Foxy 5 lysates
6 well plate experiment 1	28.272	19.375	20.419	22.738	11.150	1.273	0.844	3.546
6 well plate experiment 2	1.264	1.535	1.321	3.273	15.749	12.584	17.818	8.899

Figure 10 Normalized Signal of ATMIN and Daam2 relative to β-actin when treated with the ATM-kinase inhibitor KU55933, its vehicle control (DMSO) and Foxy 5 and its vehicle control (PBS) in 6 well plate experiment 1 (navy blue) and 6 well plate experiment 2 (red).

Figure 10 shows the data of normalized signal for ATMIN and Daam2 expression in both KU55933 and Foxy 5 treated and vehicle control in both 6 well plate experiments. ATMIN seems reduced in ½ experiments whereas Daam 2 seems to have risen in 2/2 performed in 6 well plates with KU55933 inhibitor applied. ATMIN seems reduced in 2/2 experiments whereas Daam2 seems to have risen in ½ experiments performed in the same 6 well plate experiments. However there is large variation between the controls for each experiment that any perceived changes are rendered invalid.

Experiments were also performed in T-75 flasks. Table 4 shows the normalized signal with respect to β-actin for the KU55933 inhibitor, Foxy 5 and their respective vehicles. Signal values indicated that when treated with KU55933 inhibitor, both ATMIN and Daam2 expression decreased. Alternatively when treated with Foxy 5 inhibitor, both ATMIN and Daam2 expression increased. However, the inability to calculate P values for this data means that this remains unconfirmed.

Normalised Signal of T-75 Flask experiments N=1										
ANTIBODY	ATMIN					Daam2				
Sample Type	KU 55933 Vehicle control	KU 55933 inhibitor	Foxy 5 Vehicle control	Foxy 5 inhibitor	Normal HEK 293T Cells	KU 55933 Vehicle control	KU 55933 inhibitor	Foxy 5 Vehicle control	Foxy 5 inhibitor	Normal HEK 293T Cells
Normalised Signal	137.225	27.923	13.272	20.992	144.000	197.683	56.822	94.022	235.188	675.000

Table 4.0 Normalized Signal of ATMIN and Daam2 relative to β-Actin when treated with the ATM-KINASE inhibitor KU55933, its vehicle control (DMSO) and Foxy 5 inhibitor and its vehicle control (PBS) in T75 flask experiment

Table 4.0 draws attention to the vast difference in the vehicle controls and the untreated normal HEK293T samples. These values should be similar but there is large variance suggesting inconclusive data.

Figure 11 shows the summarised normalized signal values for all the experiments relative to β-Actin.

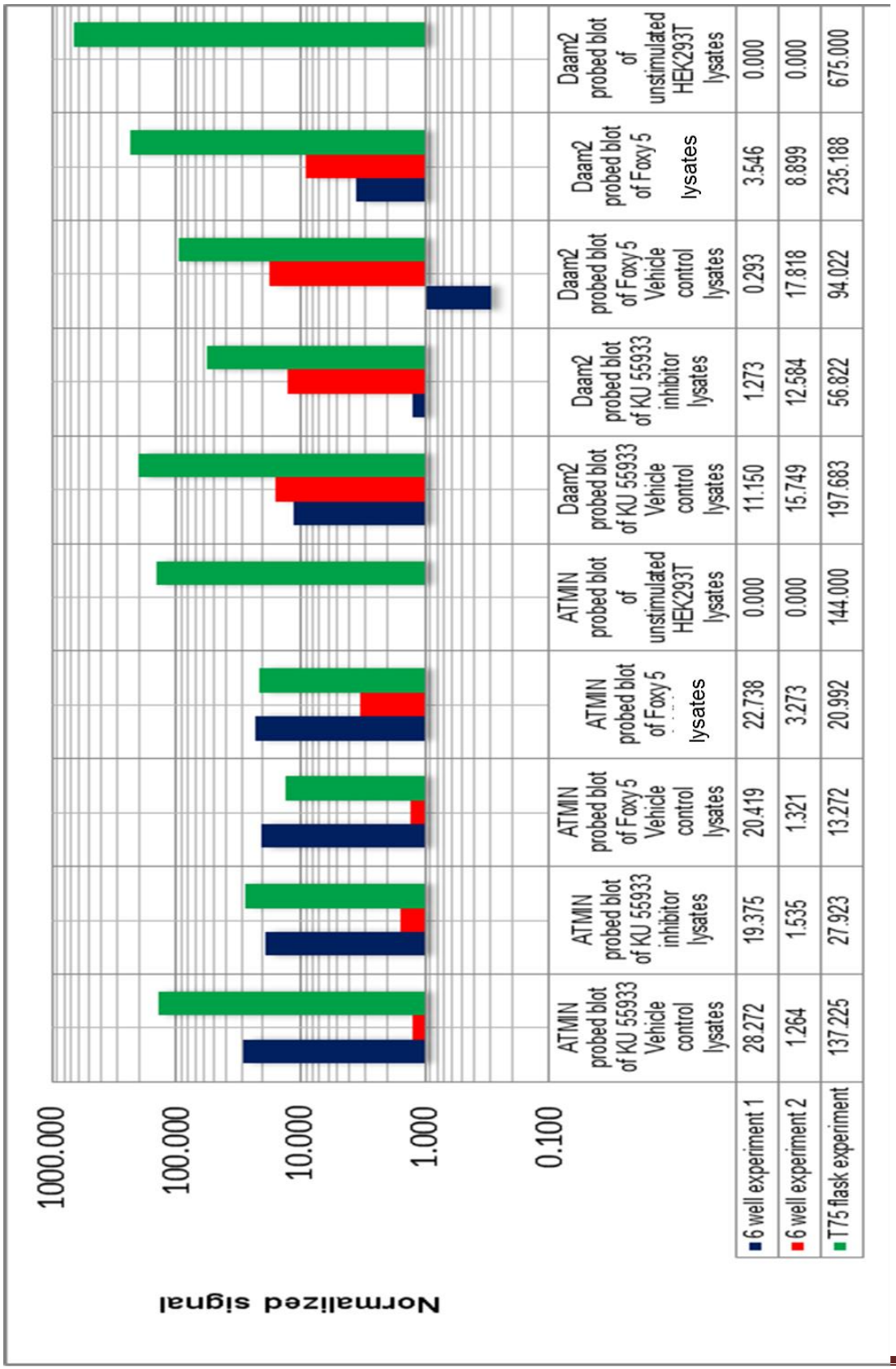

Figure 11 Summary of the normalized signal of ATMIN and Daam2 relative to β-actin when treated with the ATM-kinase inhibitor KU55933, its vehicle control (DMSO) and Foxy 5 and its vehicle control (PBS) in all experiments

3.3 Summary of effects of KU55933 and Foxy 5 on ATMIN and Daam2 compared against their own respective vehicle controls

When protein expression in KU55933 treated cells was considered alongside 0.1% DMSO as the vehicle control, both ATMIN and Daam2 expression dropped in 2/3 of experiments. Alternatively, ATMIN expression rose in all 3 experiments of Foxy 5 treated cells relative to its own vehicle control (0.1% PBS). Daam2 expression also rose in 2/3 of experiments on Foxy 5 treated cells. However, absolute ATMIN and Daam2 signal values had such a wide range of variance that p value calculation was not possible making these conclusions even more dubious.

If this data was valid so that ATMIN and Daam2 expression increased and decreased together, this may suggest that they are regulated as a pair.

3.4 Summary of effects of KU55933 and Foxy 5 on ATMIN and Daam2 compared against both vehicle controls

Typical vehicle controls should have no effect on the cells in an experiment. So if we consider the effects of these inhibitors whilst viewing vehicle controls as a whole, many of the results are inconclusive.

There were 6 experiments performed in total (two 6 well plate experiments plus one T75 experiment for KU55933 and the same for Foxy 5). ATMIN and Daam2 protein levels were between both vehicle control values in 5/6 of experiments involving KU55933. This renders KU55933 as ineffective.

Additionally Foxy 5 had no clear effects on ATMIN expression in 2/3 of the experiments or on Daam2 expression in all 3 experiments. In addition the HEK293 cells that had neither drug nor vehicle control displayed signal values much higher than in cells treated with drugs or vehicles.

3.5 Inhibition compared to confluence

Preliminary experiments on HEK293 growth included the use of the Essen Incucyte Live Cell Imaging and Analysis System to record cell growth and proliferation with video capture over the time course of the experiment (Figure 12). Cells were grown to 50-60% confluence then treated with KU55933, Foxy 5, or vehicles for 1 hour, before fresh medium was applied and the cells were returned to the incubator with video capture. Confluence was then measured over the next 70 hours. Figure 12 shows 60% reduced growth in HEK293 cells after being treated with Foxy 5 but increased proliferation by 17% after being treated with KU55933.

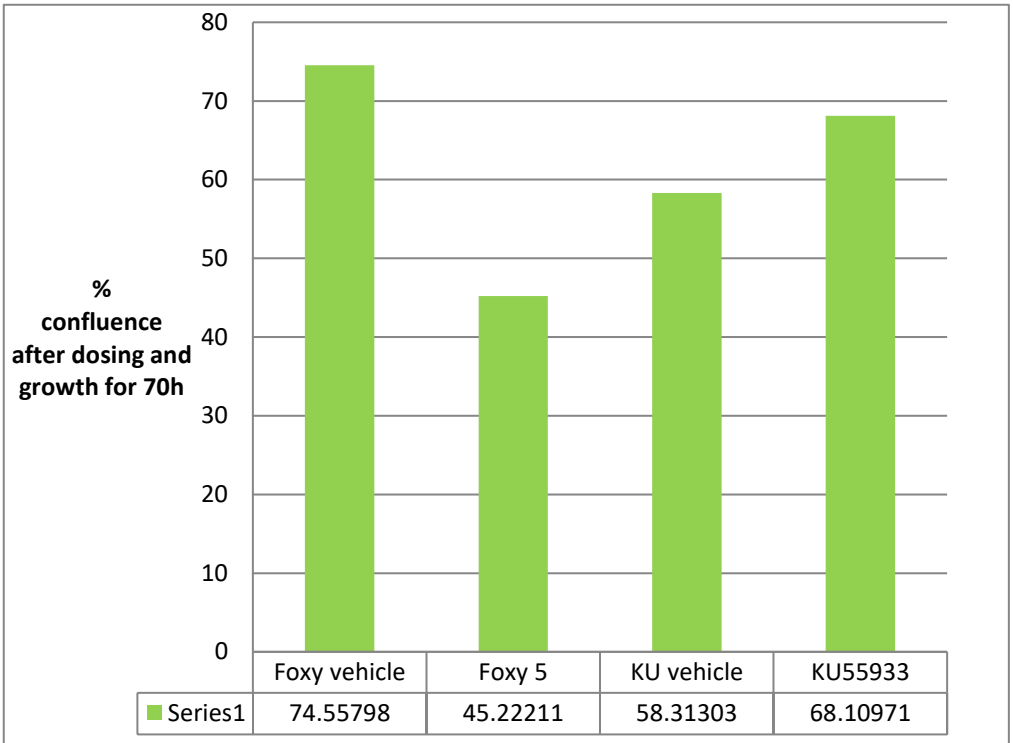

Figure 12. Confluence of HEK293T cells in 6 well plates after dosing at 1/2 confluence (40 hours) with Foxy 5 (100ng/ml), KU55933 (10µM) and related vehicle controls (DMSO and PBS respectively). N=1 each inhibitor and vehicle.

			6 well plate experiment 1		6 well plate experiment 2		T-75 Flask			
Inhibitor	Function	Cell growth	ATMIN	DAAM 2	ATMIN	DAAM 2	ATMIN	DAAM 2	Issues	Conclusion
Foxy 5 inhibitor	Wnt 5a mimicking protein	↓	↑	↓	↑	↑	↑	↑	6 well plate DAAM2 data and T-75 data do not match	Uncertain effect
KU55933 inhibitor	ATM-Kinase inhibitor	↑	↓	↓	↑	↓	↓	↓	KU55933 inhibitor treated cells had similar values to Foxy5 vehicle control	Possibly no effect

Figure 13 Summarized data of cell growth and both 6 well plate experiments along with T75 flask experimental results on ATMIN and Daam2 when treated with either Foxy 5 or KU55933 inhibitor.

Figure 13 is a summary of the effect of the KU55933 inhibitor and Foxy 5 on cell growth and on ATMIN and Daam2 expression.

Considering the 6 well experiments and the T75 flask experiments together, but crucially when considered against their own respective controls, Figure 13 shows that when treated with Foxy 5, cell growth decreased but no clear and valid conclusions could be made in regards to ATMIN and Daam2 expression.

These experiments aimed to correlate ATM kinase inhibition with cell growth and observe ATMIN/Daam2 protein levels. This is a novel study as there is no literature to suggest that ATM-kinase may impair the ability of ATMIN to bind to Daam2.

These experiments also aimed to correlate Wnt5a activation with cell growth and ATMIN and Daam2 protein expression and theorised that Wnt5a may drive a change in ATMIN/ Daam2 levels. The rationale could be pursued further in the future. An inhibition of apoptosis in HEK cells was recorded in serum-starved cultures treated with Foxy 5 (Jia et al., 2008). Experiments in this project were performed in serum-containing media so if experiments were to be repeated, it may be wise to employ serum-starved cultures also. Another study showed that Foxy5 reduced migration and invasion of 4T1 breast cancer cells without effect on growth and proliferation (Safholm, et al., 2008). This shows that it is possible to affect protein without affecting cell growth.

In summary, a matched vehicle controls analysis suggested that inhibition of ATM kinase with KU55933 (which may theoretically involve some modulation of ATMIN) was associated with no conclusive data concerning ATMIN and Daam2 protein level in HEK 293 cells. These experiments were formulated to investigate the suggested communication between ATMIN and Daam2. The idea was initially proposed from the observation that ATMIN deficient kidneys (ATMIN in Gasping 6 mutants) displayed a two-fold increase in Daam2 expression. In these experiments, the effect of KU55933 on ATMIN (as a way of "knocking it down") was difficult to judge, and the resulting effect was unclear.

When combined vehicle controls are considered as the baseline to judge the effects of the drugs against, then the results are more equivocal. While the sample size represented an excellent rate of data generation in the very short time period available, once mouse samples were withdrawn, it is too small a data set to base any valid conclusions. The safest conclusion is that, due to insufficient data, it remains to be proven what effect the drugs will have on ATMIN, Daam2 or cell growth.

3.6 Relationship between ATMIN (binding to ATM kinase) and Daam2

If there was indeed some communication between ATMIN (binding to ATM kinase) and Daam2, such that inhibition of ATM kinase led to a reduction in ATMIN and Daam2 protein level, how else might we explore this potential relationship? The next step would be to co-immunoprecipitate ATMIN with Daam2 to check for a physical interaction. Time constraints on the project did not allow for this. However, similar work was done at the beginning of the project with ATMIN and Fibrocystin using Atmin Gasping 6 four month old mouse kidney tissue lysates. Pools of nine wild type and nine heterozygous samples were used in co-immunoprecipitation experiments.

Fibrocystin is a protein localised to the cilia and is implicated in polycystic disease and the PCP pathway (Ward, 2003). At the beginning of the project, amore explorative approach was taken in that ATMIN communication with other proteins implicated in the pcp pathway such as Fibrocystin were also to be tested which is initially why Co-IP technique was performed with Fibrocystin to precipitate ATMIN protein out of solution by using ATMIN antibody. This process was used to isolate and concentrate ATMIN protein from the tissue sample containing many different proteins. If another protein such as

Fibrocystin for example, is bound to ATMIN then it would be detected via electrophoresis.

Co-immunoprecipitation was performed to purify ATMIN via immobilization of antibody-binding protein on a beaded support as detailed in the methods section. Proteins unbound to the beads were washed away. The remaining solution was run on an SDS-PAGE gel to check for the presence of ATMIN but also to identify any macromolecules that may interact with this protein. However, no significant findings were made in these experiments.

Figure 14 shows a western blot analysis of precipitated ATMIN but where a Fibrocystin antibody was applied to the blot. Though Fibrocystin is measured at 447KDa, the fusion protein possesses a band at 55kDa. So the blot presents bands between 50 and 75KDa. Assuming these are the targeted Fibrocystin band, the band in supernatant 1, has more signal than the pellet. This should not be as the most bound protein should be in the pellet elution. The only plausible explanation may be that some of the pellet was eluted whilst washing and ended up in supernatant 1 which would have been the first wash.

Finding a band for Fibrocystin in a precipitation for ATMIN suggests direct interaction between these two proteins. In relation to the project,

co-immunoprecipitation such as this could be performed with Daam2 and ATMIN as a way forward.

To check whether ATMIN and Daam2 are binding partners a co-immunoprecipitation experiment could be done. The idea would be to pulldown ATMIN, blot for Daam2 and then repeat the experiment with a pull down for Daam2 and a blot for ATMIN. If bands were seen at the expected molecular weights, it would indicate direct interaction of the proteins.

Though Co-IP is used to detect protein- protein interactions, it has its limitations such as low affinity or the inability to detect transient interaction between proteins. Co-IP technique also does not determine whether protein interaction is direct or indirect (Profacgen.com, 2017).

Alternatively, a Tandem Affinity Purification (TAP) method would be more efficient. This is also a technique used to study protein- protein interactions but involves creating a fusion protein with a designed tag on either the c terminal or the n terminal.This is especially a good system to use for low abundance protein targets such as ATMIN. Since the tag is produced for the target, this system is highly specific (Puig et al., 2001).

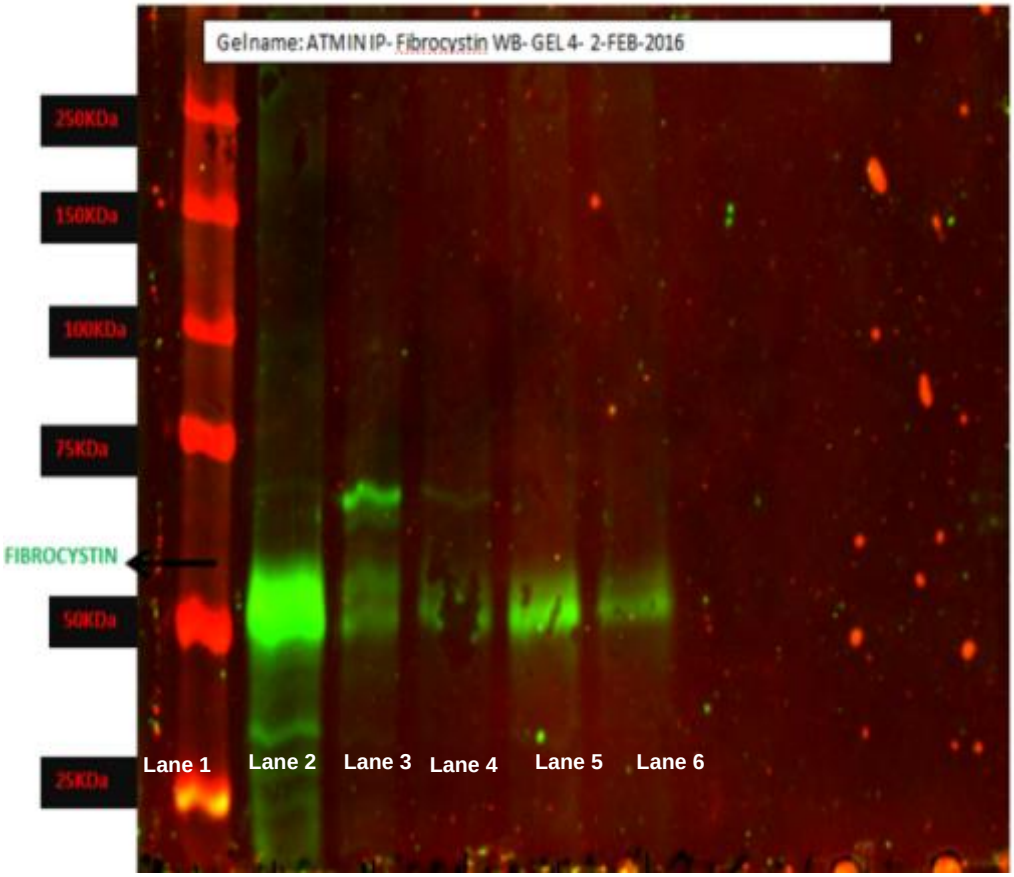

Figure 14 Western Blot of Co-immunoprecipitation of ATMIN in pooled wild type ATMIN Gasping6 4 month old mouse kidney with fibrocystin (1:200) primary antibody applied on the membrane. Lane 1: marker lane. Lane 2: ATMIN pellet. Lane 3: supernatant 1. Lane 4: supernatant 2. Lane 5: supernatant 3. Lane 6: supernatant 4.

3.7 Studies on mouse tissue

Initially, the project commenced with experiments using mouse tissue. However, the original supervisor left the university and the mouse samples were withdrawn from use. The studies on HEK 293 cells described above were instigated to pursue the investigation in the short timeframe remaining under the guidance of another supervisor.

Originally, western blot analysis was employed to measure ATMIN and Daam2 expression in wild type and heterozygous 4 month old mouse ATMIN Gasping6 kidney tissue. Figure 15 shows tissue that was lysed and run via SDS PAGE electrophoresis where proteins separated according to size. This was one of the earliest and best blots obtained from these samples. It took a very long time to tweak the western blotting protocol so that ATMIN expression would show on a blot.

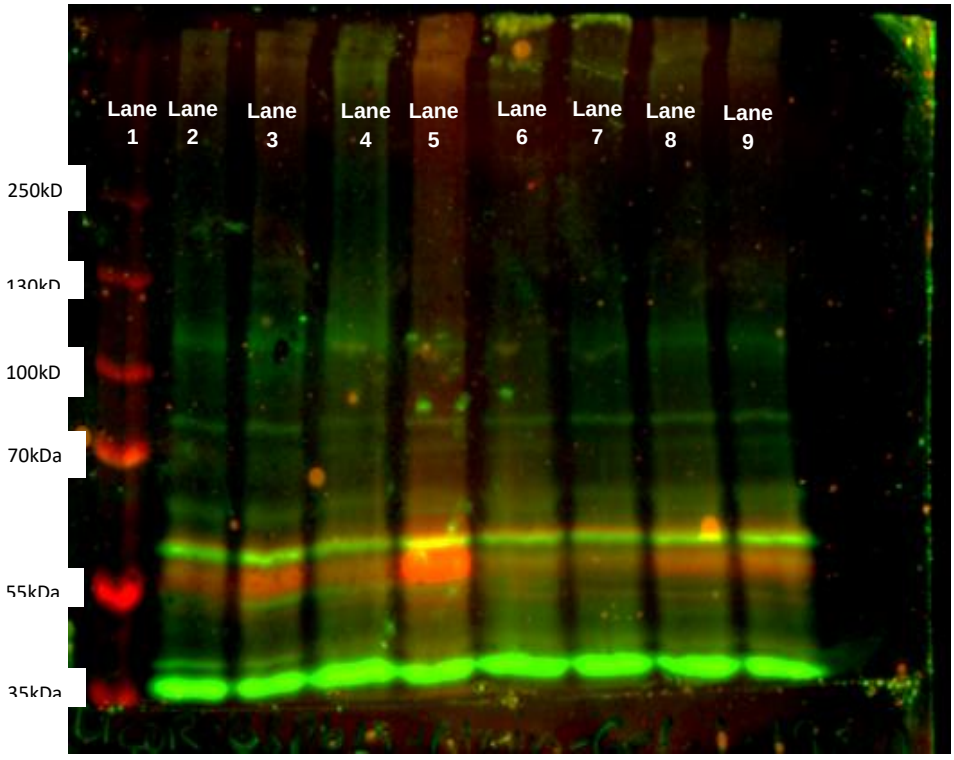

Figure 15 shows ATMIN Gasping6 4month old mouse kidney tissue WT and HET lysates on a Western blot probing for ATMIN expression (1:200) and HSP60(1:1000) as loading control. ATMIN appears at 110/120 kDa and HSP60 at 60kDa. Lane 1: Marker lane. Lane 2: 252.2F wild type. Lane 3: 260.2C wild type. Lane 4: 261. 2C wild type. Lane 5:261.2F wild type. Lane 6: 252.4B heterozygous. Lane 7: 252. 2E heterozygous. Lane 8: 261.2B heterozygous. Lane 9: 260.2A heterozygous.

Daam2 expression was also tested via western blotting in these same samples but not enough Daam2 expression was measured so there is no quantifiable data. An example of a blot obtained is shown in Figure 16**.** Samples of mouse tissue were removed from the project before further experiments could be performed on fresh lysates from these tissues.

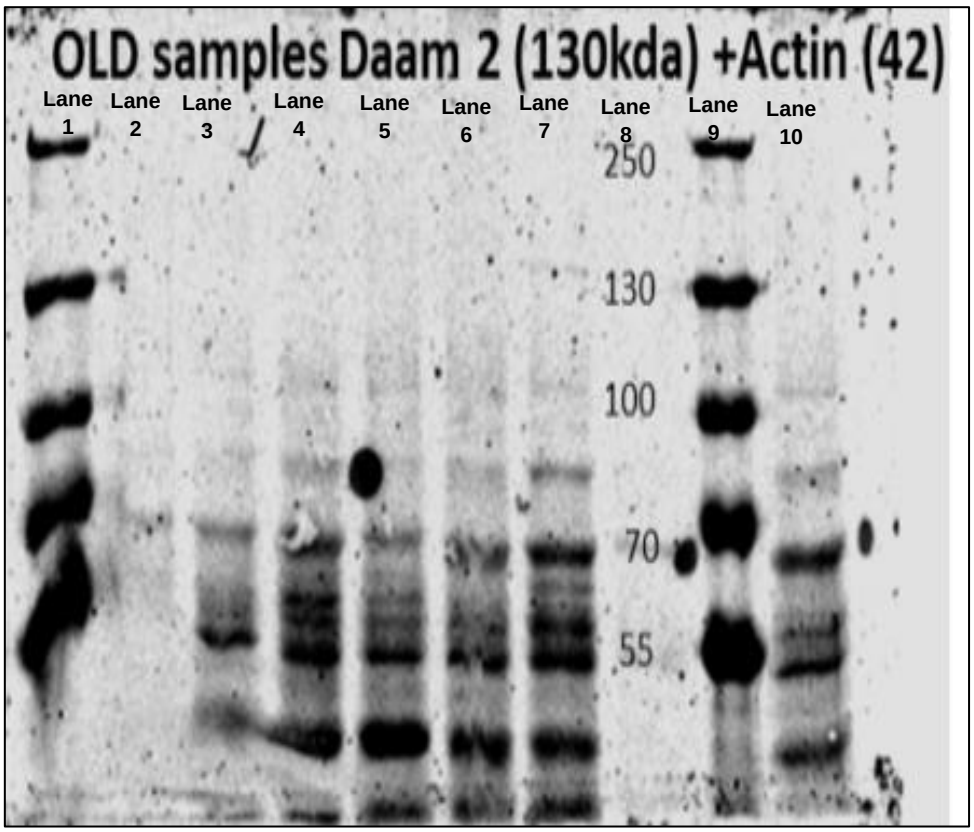

Figure 16 ATMIN Gasping6 4month old mouse kidney tissue lysates on a Western blot probing for DAAM 2 expression (1:1000, 130 kDa) and Actin (1:1000, 42 kDa) as loading control. Lanes 1 and 9: marker lanes. Lane 2: slight spill over from lane 3. Lane 3: 252.2F wild type. Lane 4: 260.2c wild type. Lane 5: 252.2c wild type. Lane 6: 260.1B wild type. Lane 7: 252.4B heterozygous Lane 8: slight spill over from lane 7. Lane 10: 248.3A heterozygous.

3.8 Summary of ATMIN and Daam2 detection in cell lines and tissues

Many Western blots were carried out to practise the western blotting technique and as troubleshooting to improve the existing protocol.

Figure 19 compared the level of RNA protein expression for ATMIN, Daam2 and Daam1 in various organs and cell lines. Close inspection of the HEK293 cell line revealed ATMIN expression is the highest whilst Daam2 is very low in comparison. Daam1 is expressed more than Daam2. This data is presented according to the Human Protein Atlas, 2017. After comparing the information in the Human Protein Atlas database, ATMIN was found to localize to nuclear bodies whilst Daam1 was localized to the cell cytosol and plasma membrane. Daam2 localized to both the nucleus and the cytosol.

In light of this information, it is easy to see why blotting for nuclear proteins like ATMIN and Daam2 can be difficult. The lysates of proteins found primarily in a sub-cellular location such as the nucleus will be more enriched in a sub-cellular fraction when compared with whole cell or tissue lysates (Sample preparation guide for western blot, Abcam, 2017). This may be useful when trying to obtain signal for protein that is weakly expressed. Using an enrichment step such as a nuclear extraction kit to draw ATMIN and Daam2 from the nucleus may maximise the signal on western blots.

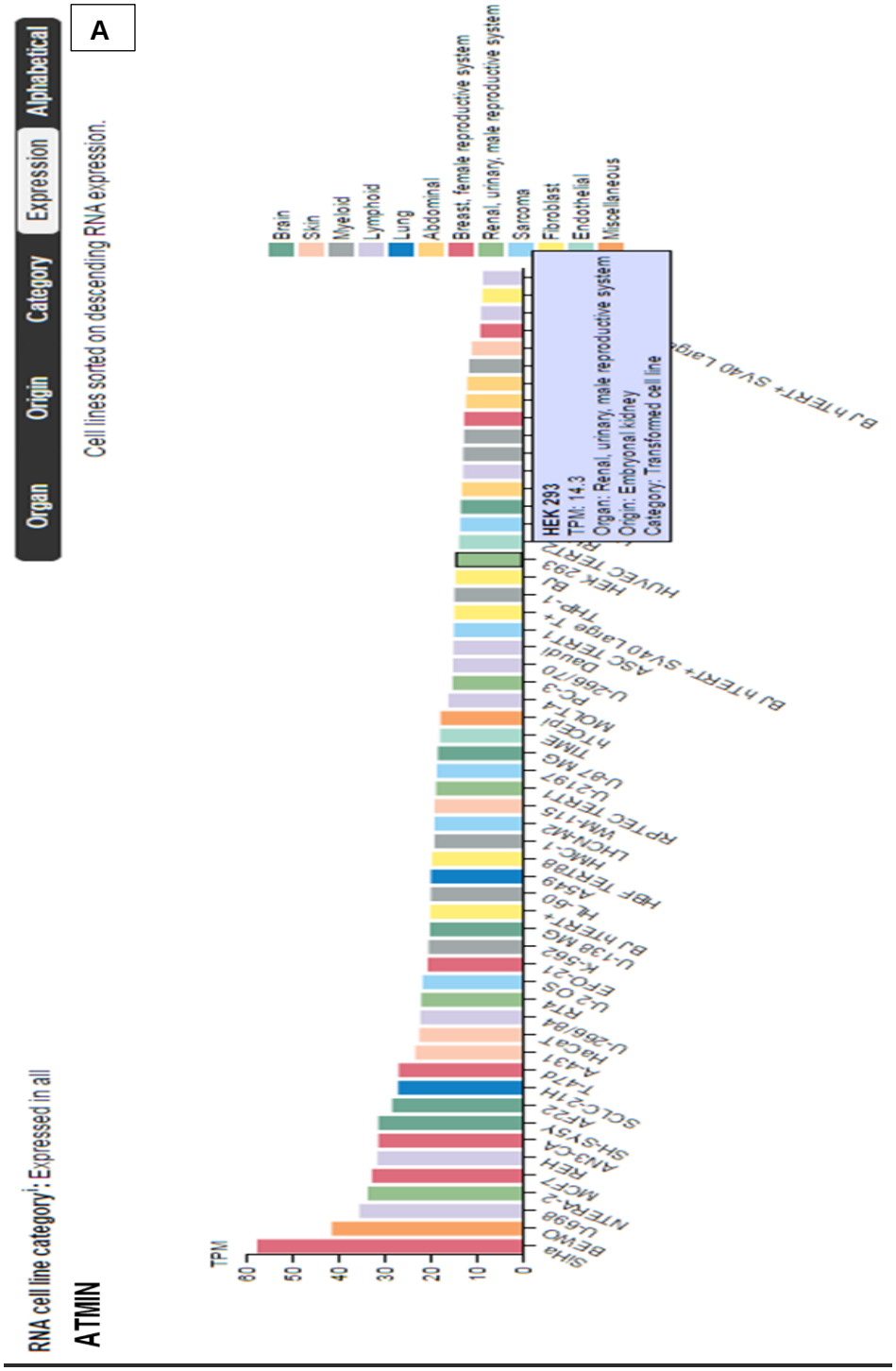

Figure 19 A) Estimated RNA protein expression in kidney, HEK 293 cells (light blue box) measured in Transcript tags per million (TPM) for ATMIN according to the Human Protein Atlas Database. From: (The Human Protein Atlas, 2017).

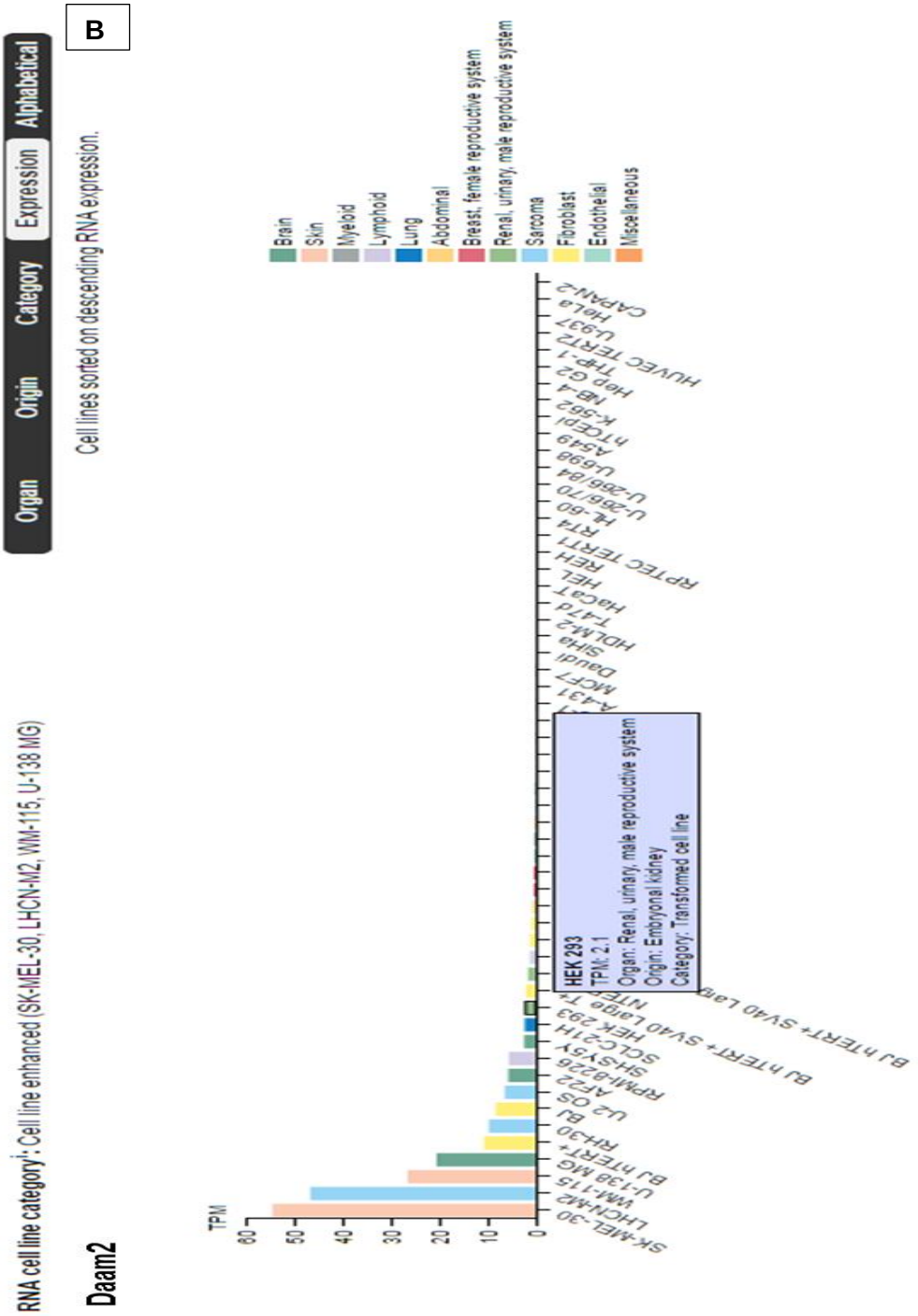

Figure 19 B) Estimated RNA protein expression in kidney, HEK 293 cells (light blue box) measured in Transcript tags per million (TPM) for Daam2 according to the Human Protein Atlas Database. From: (The Human Protein Atlas, 2017)

C

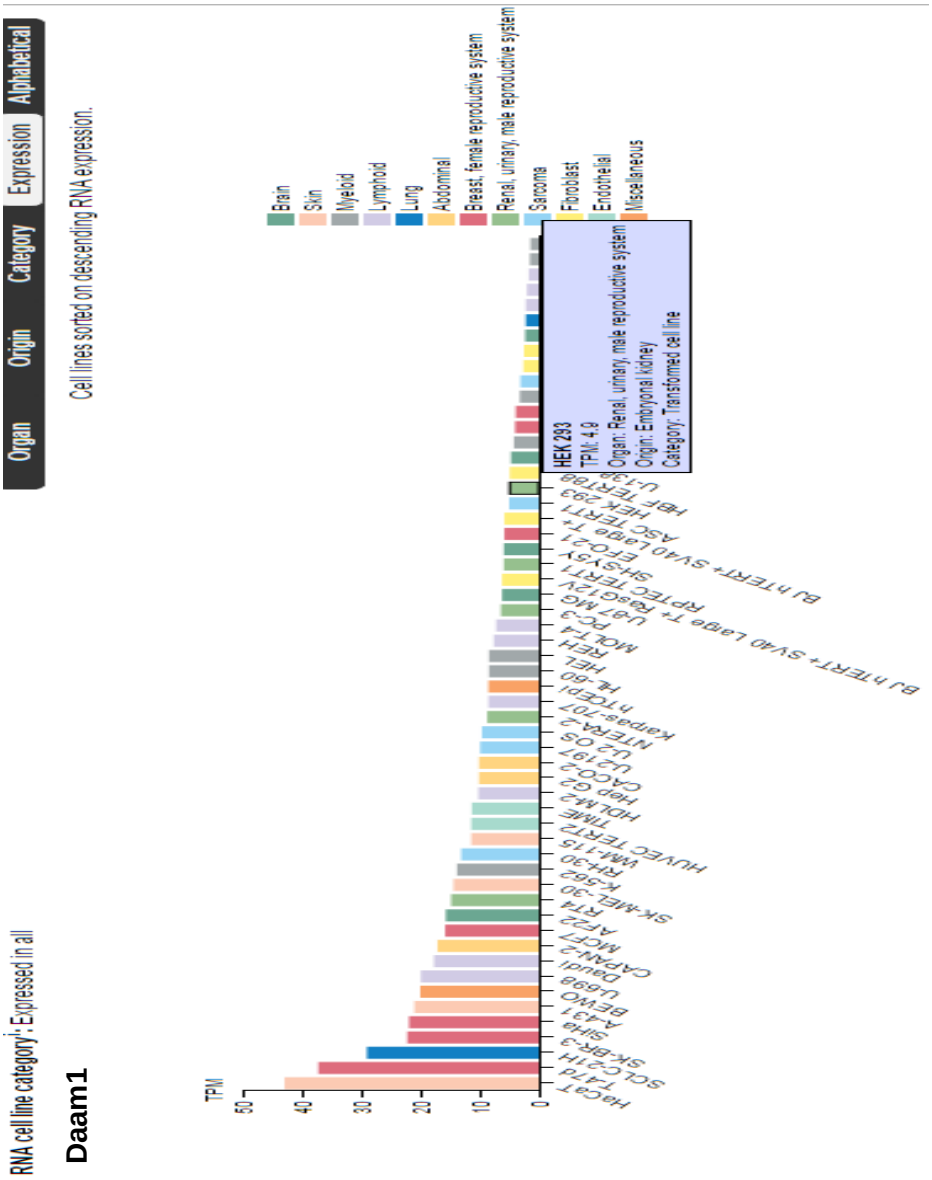

Figure 19 C) Estimated RNA protein expression in kidney, HEK 293 cells (light blue box) measured in Transcript tags per million (TPM) for Daam1 according to the Human Protein Atlas Database. From: (The Human Protein Atlas, 2017)

3.9 Daam2 localisation

A critical role for Daam2 in the developing gut was identified in previous mouse studies by Welsh, et al., 2013. The authors hypothesized that the dependence of the actin cytoskeleton on Daam2 regulation drove mesenchymal condensation thereby providing linkage of transmission of early L-R patterning signals to the forces driving gut rotation. This suggested Daam2 is important in organ morphogenesis during development.

Confocal microscopy was used to capture images of X-GAL stained embryos at embryonic week (E) E14.5 and E18.5mouse embryos. These samples were sectioned at prepared at Imperial College London. The staining was performed by PHD student Henry Lee of the Imperial College London under supervision of Dr. Charlotte Dean. My role was to take pictures of the stained sections. The embryos were from Daam2 knockout mice, a strain generated at MRC Harwell. The *E. coli* lac Z gene encodes β-galactosidase and is a widely used histochemical reporter gene. β-galactosidase catalyses the hydrolysis of X-Gal resulting in the production of a blue precipitate visualized under a microscope (Invivogen.com, 2017). A Daam2 promoter was

attached to the Lac Z reporter gene and inserted into plasmid DNA. Hydrolysis of X-Gal in the presence of β-Galactosidase revealed where Daam2 gene expression is active. Figure 20 shows the microscopy images obtained from the Daam2- Lac Z reporter mice where localization in podocytes can be seen. Strangely, Figure 21 compares E14.5 with E18.5 Daam2-Lac Z reporter mouse embryos and though no staining is seen in the E14.5 samples, E18.5 samples once more show staining suggesting DAAM2 localized to podocytes and surrounding tubules.

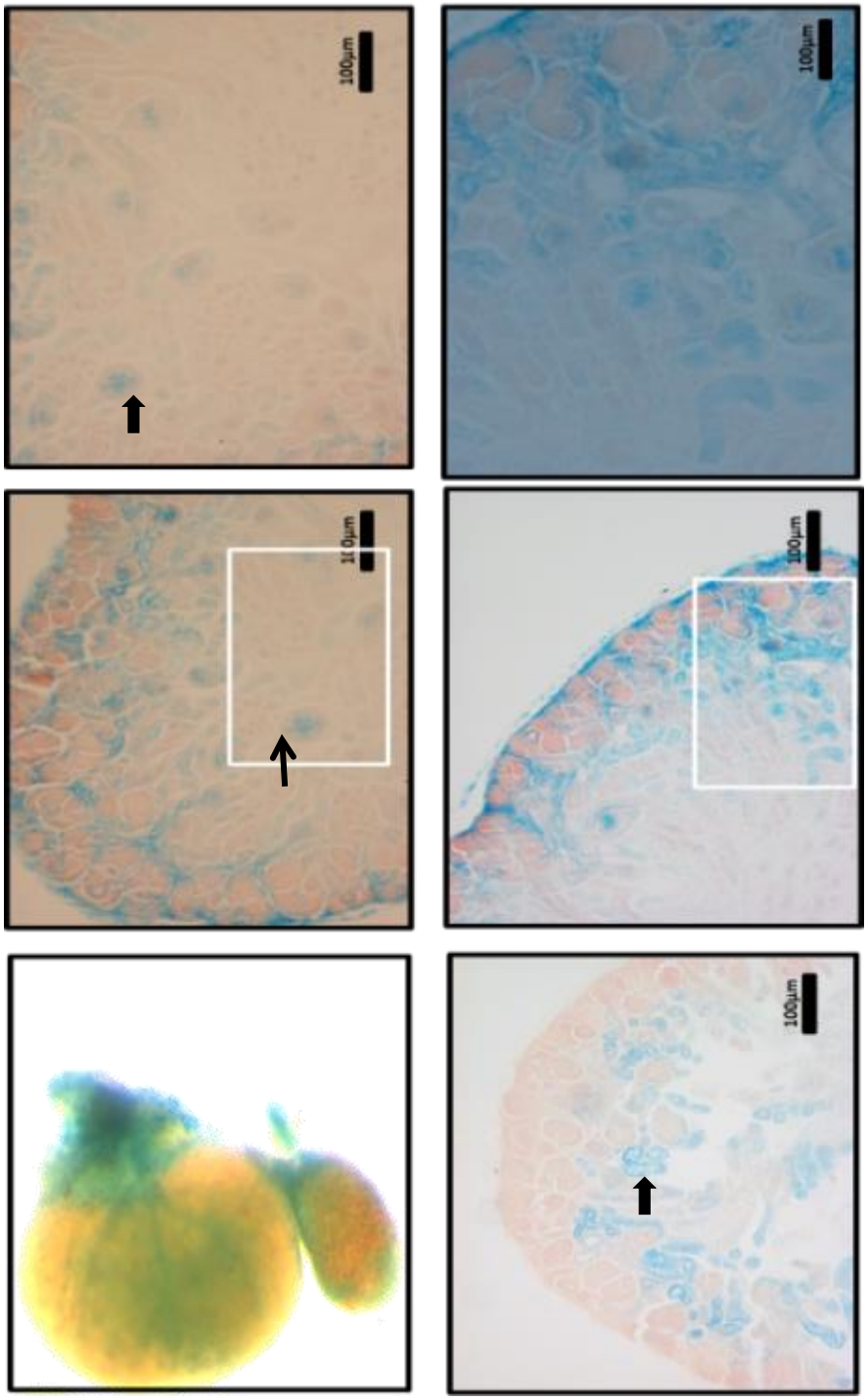

Figure 20 shows whole mount X-GAL staining of kidney tissue isolated from E18.5 Daam2-LAC Z reporter mice revealing localization of transgene expression in the presumptive ureter and localization to podocytes and surrounding tubules (blue staining and arrows).

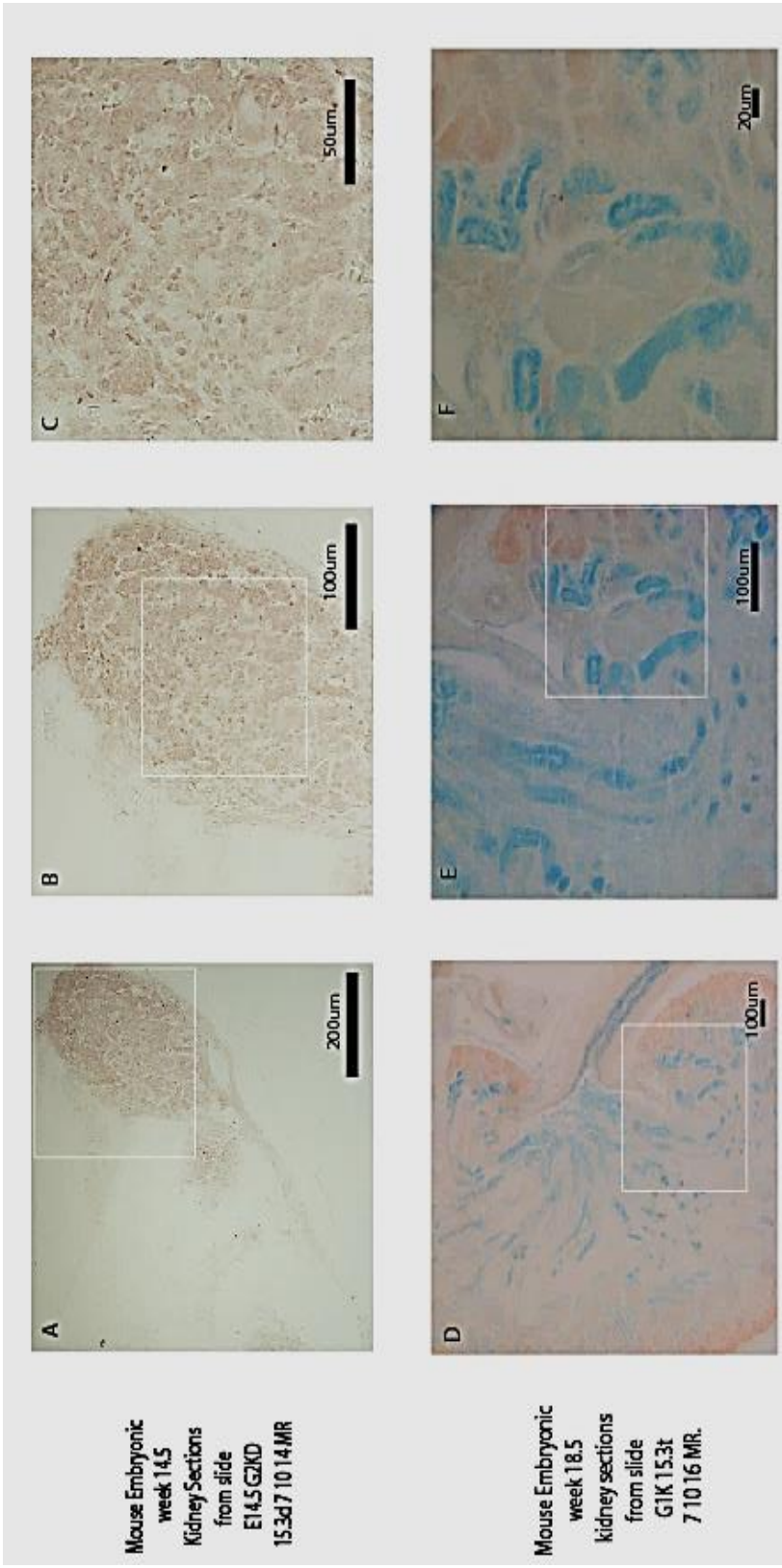

Figure 21 Shows Daam2-Lac Z staining of Mouse Embryonic week 14.5 Kidney sections from slide E14.5 G2KD 15.3d 7 10 14 MR at 10x(A) 20x (B) and 40x (C) Objective Lens. Images (C) at 4x (D) 10x and (E) at 20x Objective lens are Daam2-Lac Z stained slides of mouse Embryonic week 18.5 kidney sections from slide G1k 15.3t 10 16 MR.

To become familiar with kidney structures, images obtained from this project were compared with images from published papers. Figure 22 was used to correctly identify LacZ staining in podocyte structures.

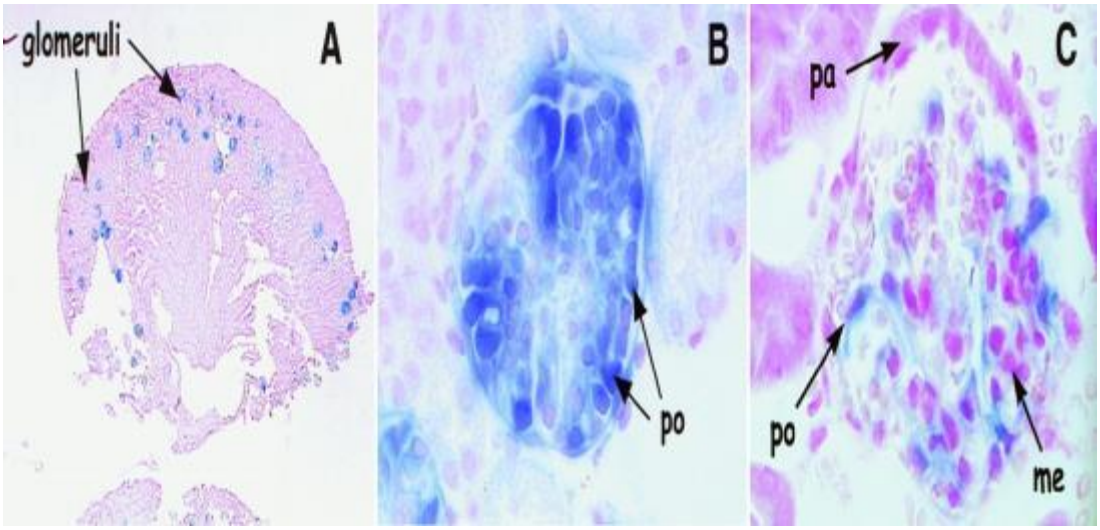

Figure 22 1.25-kb nephrin fragment-LacZ expression in the glomeruli of transgenic mouse kidneys. Embryonic day E18.5 mouse kidneys dissected, parafin embedded, sectioned and stained with β-galactosidase. Specific gene expression shown in podocytes (po, B), parietal epithelial cells (pa, C) and in mesangial cells (me, C).

From: (Wong, Cui & Quaggin, 2017)

Daam2 vasculature expression was also seen in the Daam2-LAC Z reporter mouse E18.5 staining (Figure 23). These results are consistent with other findings. According to the Genitourinary Development Molecular Anatomy Project, GUDMAP database, Daam2 is present in the kidneys and is restricted to the stroma and vasculature (Figure 24).

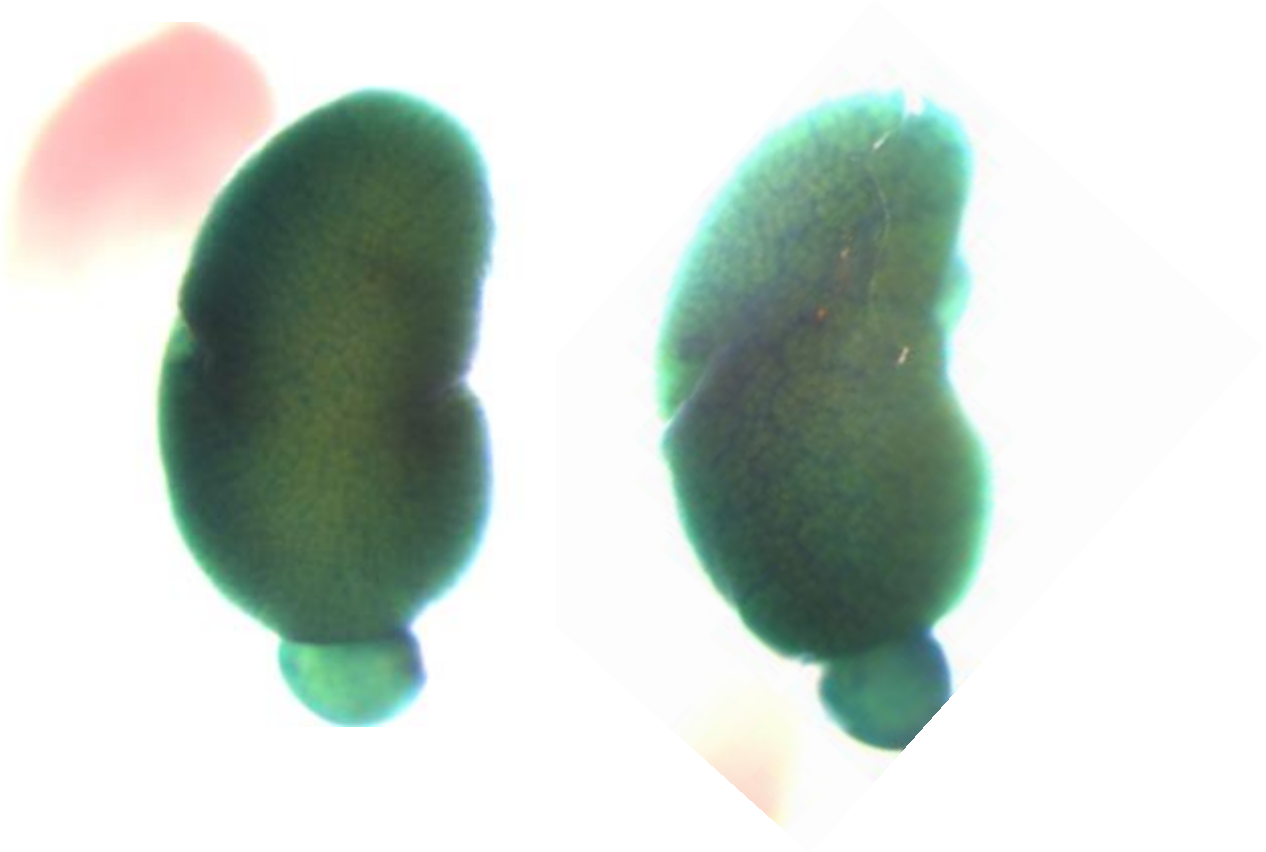

Figure 23 shows whole mount X-Gal staining of kidney tissue isolated from E18.5 Daam2- Lac Z reporter mice revealing vasculature staining.

Figure 24 Shows specific Daam2 signal in the interstitium and vasculature of a whole mouse kidney at age 15.5 days post coitum (dpc) in an In Situ Hybridization (ISH) assay. Development time=12 hours

From: GUDMAP: 10286, TS23

A comparison between Daam1, Daam2 and ATMIN expression via immunofluorescence staining in ATMIN Gasping6 four month old mouse heterozygous and wild type sections was to be made. This would provide a visual aid as to where ATMIN, Daam1 and Daam2 were being expressed in the kidneys and if there were any differences between localization in heterozygous samples compared to wild type. When ATMIN Gasping6 four month old wild type mouse kidney sections were immunostained with Daam1 antibody, basal staining was observed (Figures 25 and 26).The only difference between the images is that the experiments were performed on different days so Figure 25 was taken before Figure 26.. Sections of mouse samples were withdrawn from the project before the remaining Daam1 heterozygous samples and wild type and heterozygous samples of ATMIN and Daam2 could be stained. Hence no images are available for comparison and no valid conclusion can be made with this data.

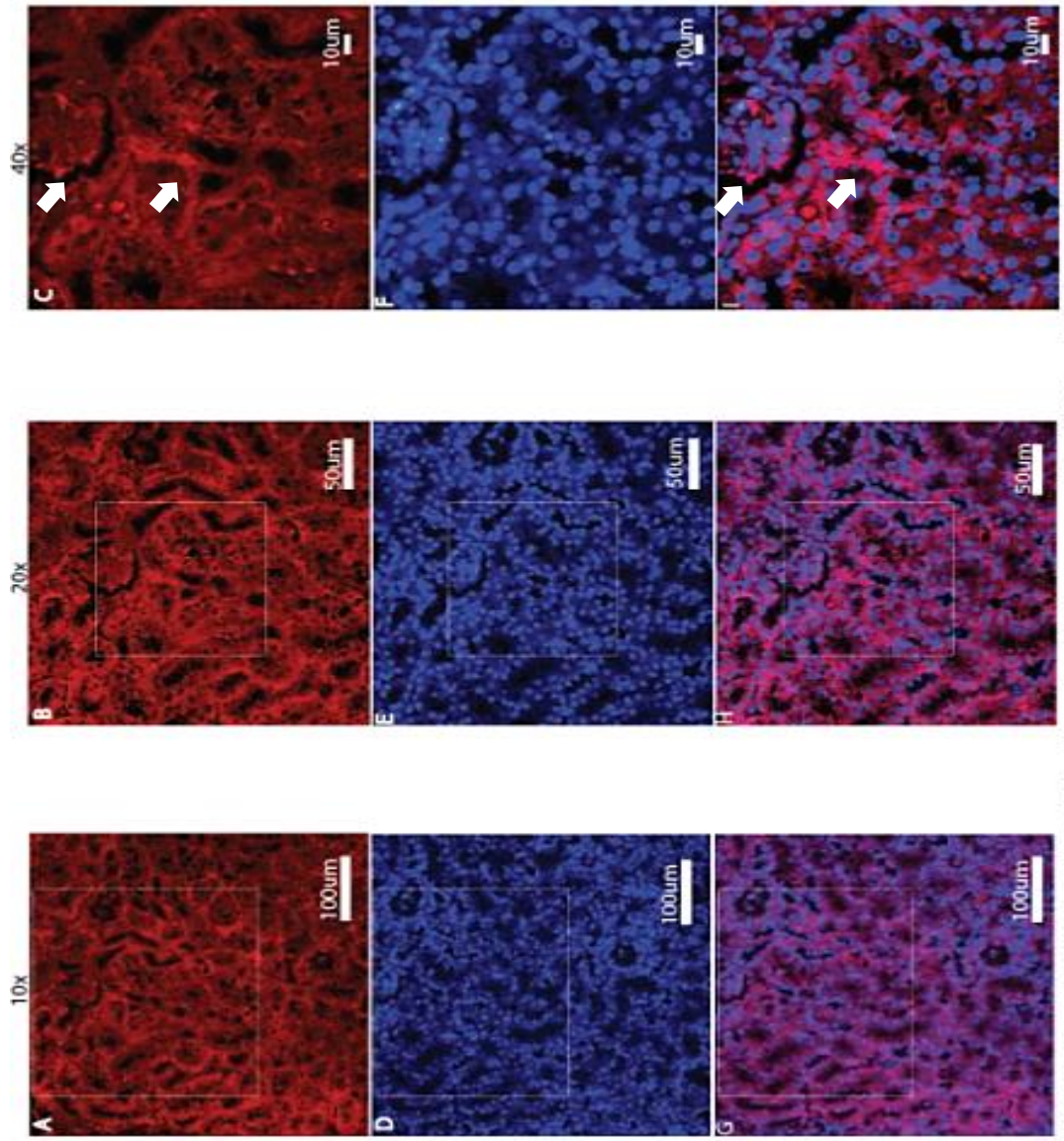

Figure 25 Slide GSP6M.252.2c.3wt.1799.15.03 labelled with anti-rabbit primary antibody Dishevelled Associated Activator of Morphogenesis 1 (DAAM1) (1:200 dil) in 4 month old Mouse Kidney sections and visualised using AlexaFluor 555 (red) conjugated antibody (A,B,C). Nuclei (blue) were stained with SlowFade® Gold Antifade Mountant using DAPI (S36938) (1:50) (D,E,F). G,H,I show each respective overlay.

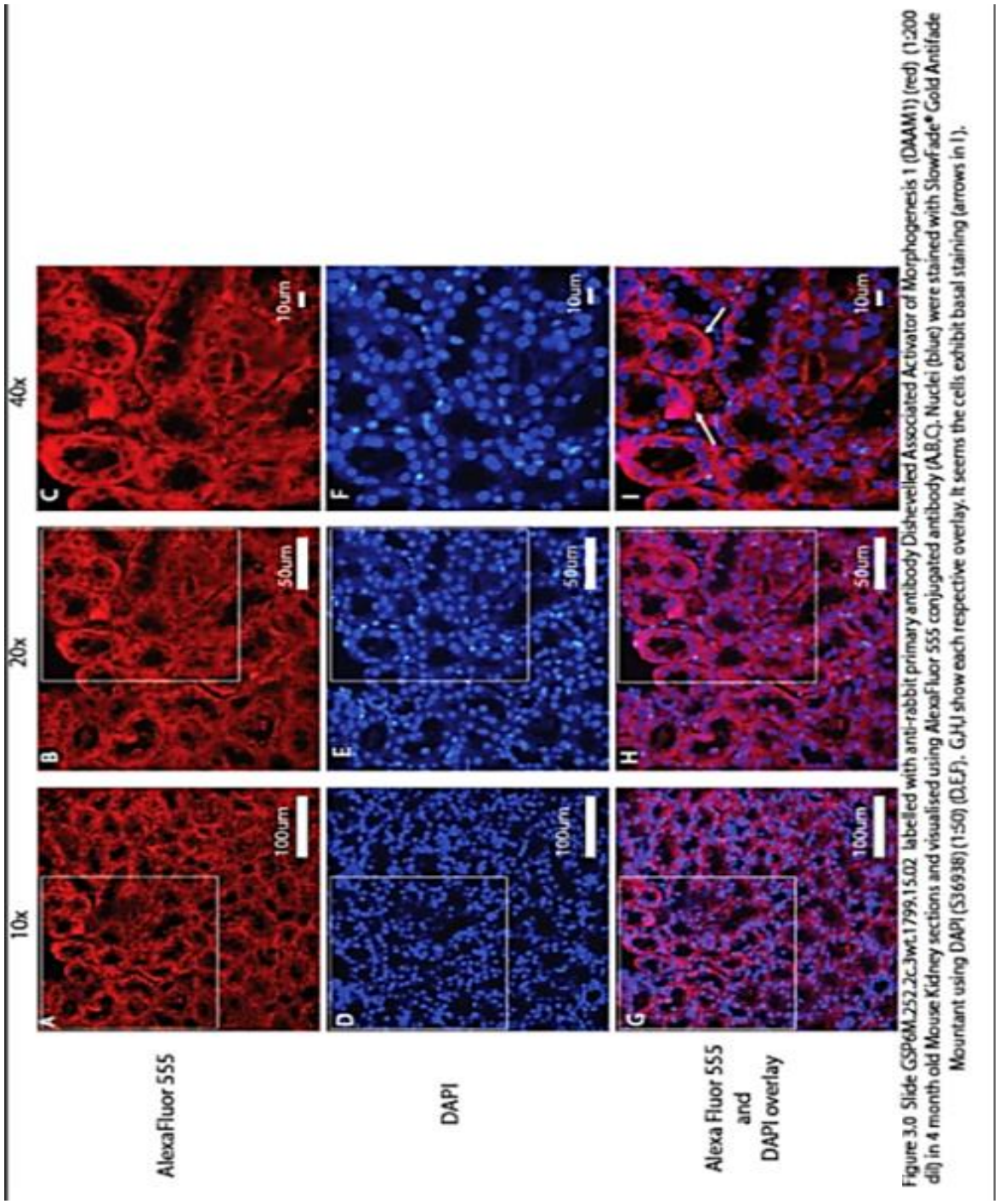

Figure 3.0 Slide GSP6M.252.2c3wt.1799.15.02 labelled with anti-rabbit primary antibody Dishevelled Associated Activator of Morphogenesis 1 (DAAM1) (red) (1:200 dil) in 4 month old Mouse Kidney sections and visualised using AlexaFluor 555 conjugated antibody (A,B,C). Nuclei (blue) were stained with SlowFade® Gold Antifade Mountant using DAPI (S36938) (1:50) (D,E,F). G,H,I show each respective overlay. It seems the cells exhibit basal staining (arrows in I).

Figure 26

4.0 DISCUSSION

HEK293 cells express ATMIN and were also shown to interact with WRN-interacting protein 1 (WRNIP1) and form a complex at sites of replication stress (Kanu, et al., 2015). In the ATMIN Gasping6 mutants expression of Daam2 was doubled (Goggolidou, 2014). This finding suggested the possibility that ATMIN may also form complexes with other proteins, e.g. Daam 1 or Daam 2. According to the Wiki-Pi human protein to protein interactions database (DBMI, 2017), no protein interactions between ATMIN and Daam2 have been reported. However, ATMIN has been shown to possess relationships with other proteins such as Vangl2 in mouse.

We proposed that an ATM kinase inhibitor such as KU55933 may possibly disrupt ATMIN thereby disrupting any ATMIN/Daam2 communication. This would theoretically impact Daam1/2 protein levels. Daam2 protein expression alone was measured following the study by (Goggolidou, et al., 2014) where Daam 2 was found upregulated but Daam 1 unchanged. However, since Daam 1 is more highly expressed in the kidneys (according to the Human Gene Database); it may be worthwhile also measuring Daam 1 protein expression.

The present study found no conclusive data on ATMIN and Daam2 expression in the presence of an ATM-kinase inhibitor.

ATMIN has been shown to have both ATM-dependent and ATM independent roles (Goggolidou & Wilson, 2016). ATM dependent roles include the initial discovery of ATMIN as a DNA damage response protein that interacted with ATM kinase protein during replicative and hypotonic stress (Kanu, et al., 2015). ATMIN ATM-independent roles were discovered when ATMIN was labelled a transcription factor when its roles in ciliogenesis and lung morphogenesis emerged (Goggolidou, et al., 2014b).

Perhaps the role of ATMIN in the kidneys is ATM-independent and the ATM-kinase inhibitor applied to the HEK 293 cells had no overall effect on ATMIN expression. If this is the case, it is less likely that any effect would be seen in Daam 2 expression since no direct links have been identified with Daam 2 and ATM interacting.

This research possesses many experimental limitations because of the pharmalogical inhibitor approach used. The inhibitor KU55933 is an ATM Kinase inhibitor that is very selective for ATM. However, inhibition of PI3K and DNA-PK occurs if the concentration of the drug falls within a certain range (16.6μM and 2.5μM respectively). Additionally also prevents the activity of mTOR when used at an IC50 of 9.3μM (Selleckchem.com, 2017). Therefore ATM kinase inhibition is dose – dependent. mTOR is an abbreviation for mechanistic target of rapamycin. It is also involved in DNA damage and can regulate other

proteins to affect cell survival and organisation of the cell cytoskeleton (Database, 2017). The dosage used in the project was 10μM which means that possibly mTOR inhibition was also occurring. Thus any results obtained would not truly represent that of only ATM kinase inhibition.

If the experiment was to be repeated, more care should be taken in making sure that the experiment is only inhibiting the target protein.

This study also presents additional limitations as there is no literature to suggest that ATMIN acts via ATM kinase in the PCP signalling pathway. It seems that the project has jumped to far ahead as a few other questions need to be investigated first such as: does ATM kinase play any role in the PCP pathway, or does ATM kinase loss impact ATMIN? In fact a more direct way to answer the true question of this thesis which is 'Does ATMIN and Daam communicate?' would be to find a more efficient way to truly inhibit ATMIN and measure response levels of Daam. One such method would be to generate a stable cell line and target a key gene to be silenced using shRNA lentivirus. This is an abbreviation for short hairpin RNA which is a type of RNA interference utilising RNA to inhibit expression of a target gene. Complementary RNA molecules are introduced into cells which bind to targeted mRNA (messenger RNA) and functionally inactivate it whilst sometimes leading to its degradation. Thus protein coded for by

the targeted mRNA fails to be produced. If shRNA expression is done through the use of Lentiviral vectors, then permanent knockdown of the target gene is provided. This is because the shRNA is passed on to daughter cells as they divide (Cellecta, Inc, 2017). This would ensure that the target protein alone is inhibited thus testing the hypothesis would be more efficient.

To further explore ATMIN and Daam2 communication, a return to previous experiments on mouse kidneys might be feasible. In the early stages of the project, ATMIN Gasping 6 heterozygous and wild type 4 month old mouse kidney tissue were lysed and proteins were separated via western blot. Inconclusive data resulted from these blots as the mouse samples were withdrawn from the project before fresh lysates could be made to run more blots. The idea was to measure the expression of ATMIN and compare it to Daam2 expression to observe whether it was increased, decreased or unchanged. It is unsure as to whether any valid results may have been obtained because literature outlines abnormal morphological defects only observed in ATMIN Gasping6 homozygous embryonic mouse kidneys. For results to be valid, ATMIN Gasping6 heterozygous 4 month mouse kidney sections would equally have to be analysed to check for morphological defects. If morphological defects were apparent and Daam2 protein expression was altered then this would suggest ATMIN and Daam2 linkage.

Alternatively if no differences were spotted, it does not eliminate the idea of communication completely. Since Daam2 was found upregulated in ATMIN Gasping6 homozygous embryonic mouse kidneys, this could indicate that Daam2 may play a larger role in embryonic development rather than mouse adulthood.

It has been suggested that Daam1 and Daam2 nucleate actin and mediate Wnt-induced cytoskeletal changes (Ajima, et al., 2015). In MDA-MB-231 human breast cancer cell monolayers Daam1 activation was induced by Wnt5a ligand (Zhu, et al., 2012). In chick, it was suggested that Daam2 may modulate formation and stabilization of Wnt/receptor complexes (Lee & Deneen, 2012). Since Daam proteins possess the ability to modulate the formation of Wnt receptor complexes perhaps Wnt5a activation may modulate ATMIN protein levels via the Daam2 upregulation.

Since Foxy 5 mimics Wnt 5a (Safholm, 2005) this study utilised it to test the effect of cell proliferation in HEK 293 cells and on ATMIN and Daam2 expression.

This study showed that a one hour treatment with the Wnt-5a–derived hexapeptide Foxy-5 resulted in reduced cell proliferation, although the data set is small.

The Daam family of proteins share conserved formin-homology (FH) and GBD domains, which are suggestive of a role in cell motility (Kida, Shiraishi & Ogura, 2004). An interesting way to further test the idea of Wnt 5a effects on cell motility would be to perform a scratch motility assay where a monolayer of cells would be treated with the Foxy 5 inhibitor for one hour. A straight line scratched across the well and the plate placed in an incucyte to observe cell (wound) repair time. This could be compared with untreated cells.

In a study performed by Kida, Shiraishi & Ogura, 2004, Daam1 demonstrated expression in mantle regions and Daam2 demonstrated expression in the ventricular zone populations in the developing spinal cord. Thus they had complementary but non-overlapping expression patterns in the developing spinal cord. According to the GUDMAP database, Daam2 is restricted to the stroma and vasculature. This correlates with the Daam2-Lac-Z reporter expression seen in kidney vasculature from the Daam2 knockout mice.

Daam2 Lac-Z staining was also seen in podocytes. Dvl2 was recruited to the plasma membrane and Daam1 moved to actin-based stress fibres when mouse and human podocytes were treated with Wnt5a. This demonstrated that PCP signalling affects podocyte shape and motility (Babayeva, Zilber & Torban, 2010).

4.1 Conclusion

It has been challenging to determine whether ATMIN directly interacts with Daam2. The study presented has merely scratched the surface of a much more complicated pathway. Although inconclusive data was obtained, increased knowledge, technical skill and ways to refine such a novel theory were gained. The suggestions outlined in section 4.0 present steps for furthering this research. The verdict cast is that there is more to explore in the ATMIN and Daam2 relationship.

5.0 References

Abraham, R. (2001) Cell cycle checkpoint signaling through the ATM and ATR kinases. *Genes & Development*. [Online] 15 (17), 2177-2196. Available from: doi:10.1101/gad.914401.

Ajima, R., Bisson, J., Helt, J. & Nakaya, M. et al. (2015) Daam1 and Daam2 are co-required for myocardial maturation and sarcomere assembly. *Developmental Biology*. [Online] 408 (1), 126-139. Available from: doi:10.1016/j.ydbio.2015.10.003.

Anon (2017)a *293T ATCC® CRL-3216™*. [Online]. 2017. Lgcstandards-atcc.org. Available from: https://www.lgcstandards-atcc.org/Products/All/CRL-3216.aspx?geo_country=gb [Accessed: 30 January 2017].

Anon (2017)b *Conservation of Planar Polarity Pathway Function Across the Animal Kingdom | Annual Review of Genetics*. [Online]. 2017. Annualreviews.org. Available from: http://www.annualreviews.org/doi/10.1146/annurev-genet-112414-055224 [Accessed: 24 March 2017].

Anon (2017)c *Foxy 5 Supplier | CAS 881188-51-8 | Tocris Bioscience | Foxy5*. [Online]. 2017. Tocris Bioscience. Available from: https://www.tocris.com/dispprod.php?ItemId=443895#.WNlbWW_yuUk [Accessed: 27 March 2017].

Babayeva, S., Zilber, Y. & Torban, E. (2010) Planar cell polarity pathway regulates actin rearrangement, cell shape, motility, and nephrin distribution in podocytes. *AJP: Renal Physiology*. [Online] 300 (2), F549-F560. Available from: doi:10.1152/ajprenal.00566.2009 [Accessed: 24 March 2017].

Bio-rad.com Western blot troubleshooting, (2017) *Western Blot Doctor - Band Size and Pattern Problems | Applications & Technologies | Bio-Rad*. [Online]. 2017. Bio-rad.com. Available from: http://www.bio-rad.com/en-uk/applications-technologies/western-blot-doctor-protein-band-size-pattern-problems#significantlyhighermw [Accessed: 29 March 2017].

Bremmer, M. (2010) Polycystic kidney disease: inheritance, pathophysiology, prognosis, and treatment. *International Journal of Nephrology and Renovascular Disease*. [Online] 69. Available from: doi:10.2147/ijnrd.s6939.

Butler, M. & Wallingford, J. (2017) Planar cell polarity in development and disease. *Nature Reviews Molecular Cell Biology*. [Online] Available from: doi:10.1038/nrm.2017.11 [Accessed: 29 March 2017].

Cellecta, Inc. (2017). *Principles of RNAi and shRNA Design - Cellecta, Inc*. [online] Available at: https://www.cellecta.com/technology-portfolio/principles-of-rnai-and-shrna-design/ [Accessed 13 Aug. 2017].

Cha, S., Tadjuidje, E., Tao, Q. & Wylie, C. et al. (2008) Wnt5a and Wnt11 interact in a maternal Dkk1-regulated fashion to activate both canonical and non-canonical signaling in Xenopus axis formation. *Development*. [Online] 135 (22), 3719-3729. Available from: doi:10.1242/dev.029025.

Database, G. (2017). *MTOR Gene - GeneCards | MTOR Protein | MTOR Antibody*. [online] Genecards.org. Available at: http://www.genecards.org/cgi-bin/carddisp.pl?gene=MTOR [Accessed 13 Aug. 2017].

DBMI, U. (2017) *Wiki-Pi*. [Online]. 2017. Severus.dbmi.pitt.edu. Available from: http://severus.dbmi.pitt.edu/wiki-pi/ [Accessed: 30 March 2017].

Dudley, J., Golovkina, T. & Ross, S. (2016) Lessons Learned from Mouse Mammary Tumor Virus in Animal Models. *ILAR Journal*. [Online] 57 (1), 12-23. Available from: doi:10.1093/ilar/ilv044 [Accessed: 23 March 2017].

Fedon, Y., Bonnieu, A., Gay, S. & Vernus, B. et al. (2012) Role and Function of Wnts in the Regulation of Myogenesis: When Wnt Meets Myostatin. *Skeletal Muscle - From Myogenesis to Clinical Relations*. [Online] Available from: doi:10.5772/48330 [Accessed: 29 March 2017].

Goggolidou, P. & Wilson, P. (2016) Novel biomarkers in kidney disease: roles for cilia, Wnt signalling and ATMIN in

polycystic kidney disease. *Biochemical Society Transactions*. [Online] 44 (6), 1745-1751. Available from: doi:10.1042/bst20160124 [Accessed: 27 March 2017].

Goggolidou, et al. (2014) Atmin mediates kidney morphogenesis by modulating Wnt signaling. *Human Molecular Genetics*. [Online] 23 (20), 5303-5316. Available from: doi:10.1093/hmg/ddu246.

Goggolidou, et al. (2014b) ATMIN is a transcriptional regulator of both lung morphogenesis and ciliogenesis. *Development*. [Online] 141 (20), 3966-3977. Available from: doi:10.1242/dev.107755 [Accessed: 24 March 2017].

Goggolidou, P. (2013) Wnt and planar cell polarity signaling in cystic renal disease. *Organogenesis*. [Online] 10 (1), 86-95. Available from: doi:10.4161/org.26766.

GUDMAP Database: Daam2 Vasculature staining, (2017) *Gudmap Gene Expression Database*. [Online]. 2017. Gudmap.org. Available from: http://www.gudmap.org/gudmap/pages/image_matrix_browse.html?gene=Daam2&symbolid=MGI%3A1923691 [Accessed: 30 March 2017].

Habas, R., Kato, Y. & He, X. (2001) Wnt/Frizzled Activation of Rho Regulates Vertebrate Gastrulation and Requires a Novel Formin Homology Protein Daam1. *Cell*. [Online] 107 (7), 843-854. Available from: doi:10.1016/s0092-8674(01)00614-6.

Heierhorst, J. (2008) Mdt1/ASCIZ: A new DNA damage response protein family. *Cell Cycle*. [Online] 7 (17), 2654-2660. Available from: doi:10.4161/cc.7.17.6593.

Hickson, I. (2004) Identification and Characterization of a Novel and Specific Inhibitor of the Ataxia-Telangiectasia Mutated Kinase ATM. *Cancer Research*. [Online] 64 (24), 9152-9159. Available from: doi:10.1158/0008-5472.can-04-2727.

Invivogen.com, (2017) *LacZ Reporter Gene System : beta-galactosidase reporter gene and kits - InvivoGen*. [Online]. 2017. Invivogen.com. Available from:

http://www.invivogen.com/lacz-reporter-gene-system [Accessed: 29 March 2017].

Jia, L., Miao, C., Cao, Y. & Duan, E. (2008) Effects of Wnt proteins on cell proliferation and apoptosis in HEK293 cells. *Cell Biology International*. [Online] 32 (7), 807-813. Available from: doi:10.1016/j.cellbi.2008.03.011 [Accessed: 26 March 2017].

Jurado, S., Conlan, L., Baker, E. & Ng, J. et al. (2011) ATM Substrate Chk2-interacting Zn2+ Finger (ASCIZ) Is a Bi-functional Transcriptional Activator and Feedback Sensor in the Regulation of Dynein Light Chain (DYNLL1) Expression. *Journal of Biological Chemistry*. [Online] 287 (5), 3156-3164. Available from: doi:10.1074/jbc.m111.306019.

Kanu, N., Zhang, T., Burrell, R. & Chakraborty, A. et al. (2015) RAD18, WRNIP1 and ATMIN promote ATM signalling in response to replication stress. *Oncogene*. [Online] 35 (30), 4009-4019. Available from: doi:10.1038/onc.2015.427 [Accessed: 27 January 2017].

Kida, Y., Shiraishi, T. & Ogura, T. (2004) Identification of chick and mouse Daam1 and Daam2 genes and their expression patterns in the central nervous system. *Developmental Brain Research*. [Online] 153 (1), 143-150. Available from: doi:10.1016/j.devbrainres.2004.07.014.

Klaus, A. & Birchmeier, W. (2008) Wnt signalling and its impact on development and cancer. *Nature Reviews Cancer*. [Online] 8 (5), 387-398. Available from: doi:10.1038/nrc2389 [Accessed: 9 March 2017].

Lee, H. & Deneen, B. (2012) Daam2 Is Required for Dorsal Patterning via Modulation of Canonical Wnt Signaling in the Developing Spinal Cord. *Developmental Cell*. [Online] 22 (1), 183-196. Available from: doi:10.1016/j.devcel.2011.10.025.

Li, Y. & Yang, D. (2010) The ATM Inhibitor KU-55933 Suppresses Cell Proliferation and Induces Apoptosis by Blocking Akt In Cancer Cells with Overactivated Akt. *Molecular Cancer Therapeutics*. [Online] 9 (1), 113-125. Available from: doi:10.1158/1535-7163.mct-08-1189.

Lienkamp, S., Liu, K., Karner, C. & Carroll, T. et al. (2012) Vertebrate kidney tubules elongate using a planar cell polarity–dependent, rosette-based mechanism of convergent extension. *Nature Genetics*. [Online] 44 (12), 1382-1387. Available from: doi:10.1038/ng.2452.

Luyten, A., Su, X., Gondela, S. & Chen, Y. et al. (2010) Aberrant Regulation of Planar Cell Polarity in Polycystic Kidney Disease. *Journal of the American Society of Nephrology*. [Online] 21 (9), 1521-1532. Available from: doi:10.1681/asn.2010010127.

MacDonald, B., Tamai, K. & He, X. (2009) Wnt/β-Catenin Signaling: Components, Mechanisms, and Diseases. *Developmental Cell*. [Online] 17 (1), 9-26. Available from: doi:10.1016/j.devcel.2009.06.016 [Accessed: 24 March 2017].

Mikels, A. & Nusse, R. (2006) Purified Wnt5a Protein Activates or Inhibits β-Catenin–TCF Signaling Depending on Receptor Context. *PLoS Biology*. [Online] 4 (4), e115. Available from: doi:10.1371/journal.pbio.0040115.

Minegishi, K., Hashimoto, M., Ajima, R. & Takaoka, K. et al. (2017) A Wnt5 Activity Asymmetry and Intercellular Signaling via PCP Proteins Polarize Node Cells for Left-Right Symmetry Breaking. *Developmental Cell*. [Online] 40 (5), 439-452.e4. Available from: doi:10.1016/j.devcel.2017.02.010.

Nakaya, M., Habas, R., Biris, K. & Dunty, W. et al. (2004) Identification and comparative expression analyses of Daam genes in mouse and Xenopus. *Gene Expression Patterns*. [Online] 5 (1), 97-105. Available from: doi:10.1016/j.modgep.2004.06.001.

Nusse, R., van Ooyen, A., Cox, D. & Fung, Y. et al. (1984) Mode of proviral activation of a putative mammary oncogene (int-1) on mouse chromosome 15. *Nature*. [Online] 307 (5947), 131-136. Available from: doi:10.1038/307131a0 [Accessed: 9 March 2017].

Otto, E., Schermer, B., Obara, T. & O'Toole, J. et al. (2003) Mutations in INVS encoding inversin cause nephronophthisis

type 2, linking renal cystic disease to the function of primary cilia and left-right axis determination. *Nature Genetics*. [Online] 34 (4), 413-420. Available from: doi:10.1038/ng1217.

Papakrivopoulou, E., Dean, C., Copp, A. & Long, D. (2013) Planar cell polarity and the kidney. *Nephrology Dialysis Transplantation*. [Online] 29 (7), 1320-1326. Available from: doi:10.1093/ndt/gft484 [Accessed: 24 March 2017].

Patel, V., Li, L., Cobo-Stark, P. & Shao, X. et al. (2008) Acute kidney injury and aberrant planar cell polarity induce cyst formation in mice lacking renal cilia. *Human Molecular Genetics*. [Online] 17 (11), 1578-1590. Available from: doi:10.1093/hmg/ddn045.

Pierce BCA Protein Assay Kit, P. (2017) *Pierce BCA Protein Assay Kit - Thermo Fisher Scientific*. [Online]. 2017. Thermofisher.com. Available from: https://www.thermofisher.com/order/catalog/product/23225 [Accessed: 30 January 2017].

Profacgen.com. (2017). *Co-Immunoprecipitation (Co-IP)*. [online] Available at: https://www.profacgen.com/Co-Immunoprecipitation-Co-IP.htm [Accessed 13 Aug. 2017].

Puig, O., Caspary, F., Rigaut, G., Rutz, B., Bouveret, E., Bragado-Nilsson, E., Wilm, M. and Séraphin, B. (2001). The Tandem Affinity Purification (TAP) Method: A General Procedure of Protein Complex Purification. *Methods*, 24(3), pp.218-229.

Rapali, P. et al. (2017). *DYNLL/LC8: a light chain subunit of the dynein motor complex and beyond*. Available from doi: 10.1111/j.1742-4658.2011.08254.x

Safholm, A., Tuomela, J., Rosenkvist, J. & Dejmek, J. et al. (2008) The Wnt-5a-Derived Hexapeptide Foxy-5 Inhibits Breast Cancer Metastasis In vivo by Targeting Cell Motility. *Clinical Cancer Research*. [Online] 14 (20), 6556-6563. Available from: doi:10.1158/1078-0432.ccr-08-0711 [Accessed: 26 March 2017].

Safholm, A. (2005) A Formylated Hexapeptide Ligand Mimics the Ability of Wnt-5a to Impair Migration of Human Breast

Epithelial Cells. *Journal of Biological Chemistry*. [Online] 281 (5), 2740-2749. Available from: doi:10.1074/jbc.m508386200.

Sample preparation guide for western blot, Abcam, (2017) *Sample preparation for western blot | Abcam*. [Online]. 2017. Abcam.com. Available from: http://www.abcam.com/protocols/sample-preparation-for-western-blot [Accessed: 29 March 2017].

Selleckchem.com. (2017). *KU-55933 (ATM Kinase Inhibitor) | ATM/ATR inhibitor | Read Reviews & Product Use Citations*. [online] Available at: http://www.selleckchem.com/products/KU-55933.html [Accessed 13 Aug. 2017].

Song, H., Hu, J., Chen, W. & Elliott, G. et al. (2010) Planar cell polarity breaks bilateral symmetry by controlling ciliary positioning. *Nature*. [Online] 466 (7304), 378-382. Available from: doi:10.1038/nature09129.

Kühn, S. and Geyer, M. (2014). *Formins as effector proteins of Rho GTPases*. Available From: doi: 10.4161/sgtp.29513

Tanegashima, K., Zhao, H. & Dawid, I. (2008) WGEF activates Rho in the Wnt–PCP pathway and controls convergent extension in Xenopus gastrulation. *The EMBO Journal*. [Online] 27 (4), 606-617. Available from: doi:10.1038/emboj.2008.9.

The Human Protein Atlas, (2017) *Cell atlas - DAAM1 - The Human Protein Atlas*. [Online]. 2017. Proteinatlas.org. Available from: http://www.proteinatlas.org/ENSG00000100592-DAAM1/cell [Accessed: 29 March 2017].

Thermofisher.com datasheet, (2017) *DAAM2 Antibody*. [Online]. 2017. Thermofisher.com. Available from: https://www.thermofisher.com/antibody/product/DAAM2-Antibody-Polyclonal/PA5-14550 [Accessed: 27 January 2017].

Thrasivoulou, C., Millar, M. & Ahmed, A. (2013) Activation of Intracellular Calcium by Multiple Wnt Ligands and Translocation of -Catenin into the Nucleus: A CONVERGENT MODEL OF Wnt/Ca2+ AND Wnt/ -CATENIN

PATHWAYS. *Journal of Biological Chemistry*. [Online] 288 (50), 35651-35659. Available from: doi:10.1074/jbc.m112.437913.

Tocris Bioscience. (2017). Cytoskeleton and Motor Proteins | Tocris Bioscience. [online] Available at: https://www.tocris.com/cell-biology/cytoskeleton-and-motor-proteins [Accessed 11 Aug. 2017].

von der Ecken, J., Müller, M., Lehman, W., Manstein, D., Penczek, P. and Raunser, S. (2014). Structure of the F-actin–tropomyosin complex. *Nature*, 519(7541), pp.114-117.

Wallingford, J. (2017) *Planar cell polarity signaling, cilia and polarized ciliary beating*. 2017.

Ward, C. (2003). Cellular and subcellular localization of the ARPKD protein; fibrocystin is expressed on primary cilia. *Human Molecular Genetics*, 12(20), pp.2703-2710.

Welsh, I., Thomsen, M., Gludish, D. & Alfonso-Parra, C. et al. (2013) Integration of Left-Right Pitx2 Transcription and Wnt Signaling Drives Asymmetric Gut Morphogenesis via Daam2. *Developmental Cell*. [Online] 26 (6), 629-644. Available from: doi:10.1016/j.devcel.2013.07.019.

Wong, M., Cui, S. & Quaggin, S. (2017) *Identification and characterization of a glomerular-specific promoter from the human nephrin gene*. [Online]. 2017. Ajprenal.physiology.org. Available from: http://ajprenal.physiology.org/content/279/6/F1027 [Accessed: 29 March 2017].

Yang, Y. (2012) Wnt signaling in development and disease. *Cell & Bioscience*. [Online] 2 (1), 14. Available from: doi:10.1186/2045-3701-2-14.

Yates, L., Schnatwinkel, C., Murdoch, J. & Bogani, D. et al. (2010) The PCP genes Celsr1 and Vangl2 are required for normal lung branching morphogenesis. *Human Molecular Genetics*. [Online] 19 (11), 2251-2267. Available from: doi:10.1093/hmg/ddq104 [Accessed: 24 March 2017].

Zhang, A., He, S., Sun, X. & Ding, L. et al. (2014) Wnt5a promotes migration of human osteosarcoma cells by triggering a phosphatidylinositol-3 kinase/Akt signals. *Cancer Cell International*. [Online] 14 (1), 15. Available from: doi:10.1186/1475-2867-14-15.

Zhu, Y., Tian, Y., Du, J. & Hu, Z. et al. (2012) Dvl2-Dependent Activation of Daam1 and RhoA Regulates Wnt5a-Induced Breast Cancer Cell Migration. *PLoS ONE*. [Online] 7 (5), e37823. Available from: doi:10.1371/journal.pone.0037823.

6.0 Appendices

6.1 Western Blotting Solutions and Gel recipes

Stock	Volume (L)	Recipe
10 x TBS	1.00	60.57g Tris , 87.66g Na Cl , pH to 7.5 , top up to 1L with distilled water
10% APS	0.05	5g APS, 50mls of distilled water
10% SDS	0.05	5g SDS, 50mls of distilled water
1 x SDS Page Running Buffer	2.00	200ml of 10 x SDS Page Running Buffer, 1800ml of distilled water
10 x SDS Page Running Buffer	1.00	30.3g Tris base, 144.1g Glycine, 10g SDS or 100ml of 10%SDS. Top up to 1L with distilled water
Semi Dry Transfer Buffer	1.00	5.82g Tris, 2.93g Glycine, 3.75ml 10%SDS, 200ml Methanol. Top up to 1L with distilled water
Wet Transfer Buffer	1.00	5.82g Tris, 2.93g Glycine, 7ml 10%SDS, 100ml Methanol Top up to 1L with distilled water
1M Tris pH 6.8	0.50	60.57g of Tris (MW 121.14), pH to 6.8, top up to 500mls with distilled water
1.5M Tris pH 8.8	0.50	90.86g of Tris (MW 121.14), pH to 8.8 top up to 500mls with distilled water
TBS/T	1.00	100ml of 10x TBS, 900ml of distilled water, 1ml Tween 20
Laemmli sample Buffer (x3 strength)	0.10	70ml Tris base pH 6.8, 6g SDS, 90mg Bromophenol Blue, 30ml Glycerol Take 9.1ml of this concoction and add 900ul B-mercaptoethanol to make 10mls of x3 strength Laemmli Sample Buffer
5% Blocking Solution	0.04	40ml TBS/T, 2g of NON-FAT milk powder
Coomassie Blue Stain	1.00	450ml Methanol, 100ml Acetic acid, 2.5g Coomassie brilliant blue R-250 . Top up to 1L with distilled water
Destain	1.00	450ml Methanol, 100ml Acetic Acid, Top up to 1L with distilled water

6.2 Table of antibody information

SDS- Page Resolving Gel	15%	12%	10%	7.5%	6%	Stacking Gel
H_2O	2.35 ml	3.35ml	4.00ml	4.85ml	5.35ml	3.4ml
1.5M Tris pH 8.8	2.50 ml	2.50ml	2.50ml	2.50ml	2.50ml	-
1M Tris pH 6.8	-	-	-	-	-	630ul
30% Protogel Acrylamide	5.00 ml	4.00ml	3.34ml	2.50ml	2.00ml	750ul
10% SDS	100ul	100ul	100ul	100ul	100ul	50ul
10% APS	80ul	80ul	80ul	80ul	80ul	50ul
TEMED	8ul	8ul	8ul	8ul	8ul	8ul

Technique	Description	Host Species	Name	Dilution factor	Final Volume in diluent	Molecular weight (kDa)	Manufacturer
Western Blotting	Primary Antibodies	Rabbit	Daam 1	1/500	20ul	130	Thermofisher, (Invitrogen)
			Daam 2	1/500	20ul	130	Thermofisher, (Invitrogen)
			Atmin	1/200	50ul	110,120	Millipore
			Atmin	1/200	50ul	110,120	Cambridge Bioscience
			Inversin	1/200	50ul	118	Abcam
	House keeping protein	Mouse	HSP60	1/1000	10ul	61	Abcam
			Actin	1/1000	10ul	42	Thermofisher
	Secondary Antibodies	Donkey	Anti-Rabbit	1/10000	1	N/A	LICOR
			Anti-Mouse	1/10000	1	N/A	LICOR
Immuno-Fluorescence	Primary Antibodies	Rabbit	Daam 1	1/200	0.5ul	N/A	Thermofisher, (Invitrogen)
			Daam 2	1/200	0.5ul	N/A	Thermofisher, (Invitrogen)
	Secondary Antibody	Goat	Anti-Rabbit IgG-H&L Alexa Fluor555	1/1000	0.1ul	N/A	Abcam